# Application of the PML Absorbing Layer Model to the Linear Elastodynamic Problem in Anisotropic Heteregeneous Media

Francis Collino, Chrysoula Tsogka

INRIA

INSTITUT NATIONAL DE RECHERCHE EN INFORMATIQUE ET EN AUTOMATIQUE

# *Application of the PML absorbing layer model to the linear elastodynamic problem in anisotropic heteregeneous media*

Francis COLLINO, Chrysoula TSOGKA

**N ° 3471**

Août 1998

THÈME 4


ISSN 0249-6399

INRIA
ROCQUENCOURT

# Application of the PML absorbing layer model to the linear elastodynamic problem in anisotropic heteregeneous media

Francis COLLINO*, Chrysoula TSOGKA†

Thème 4 — Simulation et optimisation
de systèmes complexes
Projet Ondes

Rapport de recherche n ° 3471 — Août 1998 — 28 pages

**Abstract:** We present and analyze a perfectly matched absorbing layer model for the velocity-stress formulation of elastodynamics. This layer has the astonishing property of generating no reflection at the interface between the free medium and the artificial absorbing medium. This allows us to obtain very low spurious reflection even with very thin layers. Several experiments show the efficiency and the generality of the model.

**Key-words:** absorbing layers, absorbing conditions, mixed finite elements, anisotropic

*(Résumé : tsvp)*

* INRIA-rocquencourt. Eliane.Becache@inria.fr
† INRIA-rocquencourt. Chrysoula.Tsogka@inria.fr

Unité de recherche INRIA Rocquencourt
Domaine de Voluceau, Rocquencourt, BP 105, 78153 LE CHESNAY Cedex (France)
Téléphone : 01 39 63 55 11 - International : +33 1 39 63 55 11
Télécopie : (33) 01 39 63 53 30 - International : +33 1 39 63 53 30

# Application du modèle de couches absorbantes parfaitement adaptées (PML) au problème de l'élastodynamique linéaire en milieu hétérogène anisotrope

**Résumé :** Nous présentons et analysons un modèle de couches absorbantes parfaitement adaptées (PML) pour la formulation en vitesse-contraintes de l'élastodynamique. Ce modèle a la propriété étonnante de ne générer aucune réflection parasite à l'interface entre le milieu élastique et la couche absorbante. Ceci nous permet d'obtenir des réflections très faibles même dans le cas de couches fines. Plusieurs expériences numériques montrent l'efficacité et la généralité du modèle.

**Mots-clé :** couches absorbantes, conditions absorbantes, élastodynamique, éléments finis mixtes, anisotropie

# Table of Contents



# 1 Introduction

The simulation of waves by finite-differences or finite-elements methods in unbounded domains requires a specific treatment for the boundaries of the necessarily truncated computational domain. Two solutions have been proposed for this purpose : absorbing boundary conditions (ABC) and absorbing layers. ABC's have been introduced by B. Engquist and A. Majda for the acoustic wave equation [11]. They consist in adding to the wave equation some suitable local boundary conditions that simulate the outgoing nature of the waves impinging on the borders. This method works particularly well for absorbing waves nearly normally incident to the artificial boundaries. For waves traveling obliquely, higher order ABC must be used to achieve acceptable accuracy, [12].

For elastic waves, the situation is more complex. First, the transparent condition, i.e. the exact condition relating normal stress and displacement on a line for outgoing waves, is no longer a scalar but a matrix integro-differential relation. Its approximation by partial differential equations, which is the usual way to make ABC, leads to a very complex system of equations, especially for higher order methods. The stability of the coupled problem composed of the elastodynamic system completed with these artificial conditions is then very difficult to analyze and the situation is even more intricate when discretization is considered, [8]. To overcome these difficulties, Higdon [14], [16], proposed to combine several first order boundary conditions designed for the wave equation, each of them being associated with either the pressure waves velocity or the shear waves velocity. These conditions are theoretically stable, [15], relatively easy to implement and efficient for the waves traveling in a direction close to the normal of the artificial boundaries. They can be adapted to the case of surface waves too, [21]. However, for other directions of propagation, important spurious reflections may occur. Some authors, [18] for instance, have proposed to optimize the coefficients of Higdon's method in order to make these reflections decrease. However, numerical experiments still show relatively strong spurious reflections in some situations and stability problems when higher order numerical schemes are used, [20].

Layers models are an alternative to ABC. The idea is to surround the domain of interest by some artificial absorbing layers in which waves are trapped and attenuated. For elastic waves, several models have been proposed. For instance, Sochacki et al., [21] suggest to add inside the layers some attenuation term, proportional to the first time derivative of the displacement to the elastodydamic equations. This technique is inspired by Physics and revealed to be quite delicate in practice. The main difficulty is that, when entering the layers, the waves "sees" the change in impedance of the medium and then is reflected artificially into the domain of

interest. The use of smooth and not too high attenuation profiles allows us to weaken the difficulty but require the use of thick layers, [17].

In this paper, we propose to adapt a layer technique introduced in [5] for the Maxwell's equations by Bérenger and that is now the most widely used method for the simulation of electromagnetic waves in non bounded domains, [6], [7], [23] . This technique consists in designing an absorbing layer called perfectly matched layer (PML) that possesses the astonishing property of generating no reflection at the interface between the free medium and the artificial absorbing medium. This property allow us to use a very high damping parameter inside the layer and consequently a small layer width while achieving a quasi-perfect absorption of the waves. To our knowledge, this method has been already used only once for elastic waves simulation. In [13], the authors propose the use of PML for the compressionnal and shear potentials formulation. In our paper, the PML are incorporated in the stress-velocity formulation.

The present paper is organized as follows. In section 2 we construct the PML model in the general case of an evolution problem. It is based on an interpretation of the PML model of Bérenger [5] as a change of variable in the complex plane c.f [9], [19]. In section 3, we apply the previous model to the velocity stress formulation for elastodynamics and we study the properties of the continuous PML model via a plane wave analysis. In order to show the generality of the PML model, two numerical schemes are presented (section 4). The first one is the classical Virieux finite-differences scheme [22] while the second one is a mixed finite-element scheme [3] which allow us to consider anisotropic media as well. We then study in section 5 the properties of the discrete model in the case of the finite element scheme in terms of a numerical dispersion analysis. Finally in section 6 we present several numerical results which show the efficiency of this model even in the case of heterogeneous, anisotropic elastic media and its superiority when compared to the classical ABC's conditions.

## 2 Pml model for a general evolution problem

We will present in this section the basic principles of the P.M.L model in the general case of an evolution problem. This will allow us to generalize it to other models of wave propagation. Consider a general evolution problem of the following form, posed initially in the space $\mathbb{R}^m$

$$(1)\qquad \begin{aligned} &(a)\quad \partial_t v - A\partial_x v - B\partial_y v = 0 \\ &(b)\quad v(t=0) = v_0\ , \end{aligned}$$

where $v$ is a $m$-vector, $A$ is a $m \times m$ matrix and $B\partial_y = \sum_{j=2}^{n} B_j \partial_{y_j}$ with $B_j$ some $m \times m$ matrices. Moreover, we assume that the initial condition $v_0$ is supported in $\mathbb{R}^n_- = \{(x, y_2, .., y_n) \in \mathbb{R}^n,\ x < 0\}$ as shown in Figure 1.

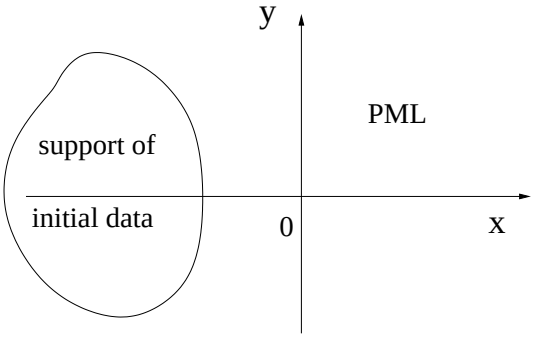


Figure 1: Geometry of the problem.

We would like to replace problem (1) by an equivalent one posed in the left half-space. Following the basic principle of the PML model, that is *to couple the equation in the left half-space with an equation in the right half-space such that there is* **no reflection** *at the interface and that the wave* **decreases exponentially** *inside*

*the layer.* We first introduce the following system

$$
\begin{aligned}
& v = v^{\parallel} + v^{\perp} \\
& \partial_t v^{\parallel} - B\partial_y v = 0 \\
& \partial_t v^{\perp} - A\partial_x v = 0 \ ,
\end{aligned}
\tag{2}
$$

where index $\parallel$ means that we keep only the derivative parallel to the interface, i.e. the $y$-derivative (while index $\perp$ means that only the $x$-derivative is considered). It is easy to see that system (2) is equivalent to(1)-(a). Secondly we introduce some positive scalar function $d(x)$, which will play the role of the damping factor and we define a new wave, $u$, solution of (1)-(a) in the left half-space and satisfying a new system in the right half-space, involving a damping on the normal component, so that $u$ satisfies

$$
\begin{aligned}
& \partial_t u - A\partial_x u - B\partial_y u = 0, \quad x < 0 \\
& u(t=0) = v_0, \quad x < 0 \ ,
\end{aligned}
\tag{3}
$$

and

$$
\begin{aligned}
& u = u^{\parallel} + u^{\perp} \\
& \partial_t u^{\perp} + d(x)u^{\perp} - A\partial_x u = 0, \quad x > 0, \\
& \partial_t u^{\parallel} - B\partial_y u = 0, \quad x > 0, \\
& u(t=0) = 0, \quad x > 0 \ .
\end{aligned}
\tag{4}
$$

Another way to set the PML model is to assume that $d(x)$ is extended by zero in $\mathbb{R}^n_-$

$$
d(x) = 0, \quad \forall x \leq 0 \ ,
$$

and that $(u^{\parallel}, u^{\perp})$ is sought in $\mathbb{R}^n$ solution of

$$
\begin{aligned}
& \partial_t u^{\perp} + d(x)u^{\perp} - A\partial_x u = 0 \\
& \partial_t u^{\parallel} - B\partial_y u = 0 \\
& u(t=0) = v_0 \\
& \text{with } u = u^{\parallel} + u^{\perp} \ .
\end{aligned}
\tag{5}
$$

If we look for the stationary solutions of system (1) with frequency $\omega$, we get

$$
i\omega\hat{v} - A\partial_x\hat{v} - B\partial_y\hat{v} = 0 \ .
$$

In the same way, the stationary solutions of system (5), satisfy

$$
\begin{aligned}
& (i\omega + d(x))\hat{u}^{\perp} - A\partial_x\hat{u} = 0 \\
& i\omega\hat{u}^{\parallel} - B\partial_y\hat{u} = 0 \\
& \text{with } \hat{u} = \hat{u}^{\parallel} + \hat{u}^{\perp} \ ,
\end{aligned}
$$

or, equivalently

$$
\begin{aligned}
& i\omega\hat{u}^{\perp} - \frac{i\omega}{i\omega + d(x)} A\partial_x\hat{u} = 0 \\
& i\omega\hat{u}^{\parallel} - B\partial_y\hat{u} = 0 \\
& \text{with } \hat{u} = \hat{u}^{\parallel} + \hat{u}^{\perp} \ .
\end{aligned}
$$

We can remark now, that $\hat{u}$ and $\hat{v}$, satisfy the same equations in the area where $d$ is zero, whereas inside the layer, the PML model consist in the simple substitution

$$
\partial_x \rightarrow \partial_{\tilde{x}} = \frac{i\omega}{i\omega + d(x)}\partial_x \ ,
$$

which implies the complex change of variables

$$\tilde{x}(x) = x - \frac{i}{\omega}\int_0^x d(s)ds \ .$$

We can study now the properties of this model using a plane wave analysis. We seek particular solutions of system (1) in the following form

$$\begin{aligned} &v = v_0 e^{-i(k_x x + k_y y - \omega t)},\ v_o \in \mathbb{R}^m \\ &k = (k_x, k_y) \in \mathbb{R}\times\mathbb{R}^{n-1},\ \omega \in \mathbb{R}\ . \end{aligned} \tag{6}$$

Formula (6) is a plane wave propagating in the direction $k$ with the phase velocity $\omega/|k|$. In order to be a solution of problem (1), $V$ has to satisfy the following relations

$$iv_0\omega - iAv_0k_x - iBv_0k_y = 0\ . \tag{7}$$

In the same way, we seek particular solutions of system (5) in the following form

$$\begin{aligned} u^{\parallel} &= a^{\parallel} e^{-i(k_x \tilde{x}(x) + k_y y - \omega t)} \\ u^{\perp} &= a^{\perp} e^{-i(k_x \tilde{x}(x) + k_y y - \omega t)} \\ u &= u^{\parallel} + u^{\perp}\ . \end{aligned}$$

In order to be a solution of problem (5), $u^{\parallel}$ and $u^{\perp}$ have to satisfy the following relations

$$\begin{aligned} &ia^{\parallel}\omega - iB(a^{\perp} + a^{\parallel})k_y = 0 \\ &(i\omega + d(x))a^{\perp} - i\left(1 - \frac{id(x)}{\omega}\right)A(a^{\perp} + a^{\parallel})k_x = 0\ , \end{aligned} \tag{8}$$

or, equivalently

$$\begin{aligned} &ia^{\parallel}\omega - iB(a^{\perp} + a^{\parallel})k_y = 0 \\ &ia^{\perp}\omega - iA(a^{\perp} + a^{\parallel})k_x = 0\ . \end{aligned} \tag{9}$$

Adding the two equalities of (9), gives

$$i(a^{\perp} + a^{\parallel})\omega - iA(a^{\perp} + a^{\parallel})k_x - iB(a^{\perp} + a^{\parallel})k_y = 0\ . \tag{10}$$

We can remark now that if we chose $a^{\perp}$ and $a^{\parallel}$ such that

$$a^{\perp} + a^{\parallel} = v_0,$$

equation (10) becomes the same as (7). Moreover from (9) we get

$$a^{\parallel} = Bv_0\frac{k_y}{\omega}, \qquad a^{\perp} = Av_0\frac{k_x}{\omega}\ , \tag{11}$$

which gives the plane wave solution of (5). We then have the following property:
*The plane wave $U$ solution of system (5) can be written in the form*

$$u \quad = v_0\ e^{-i(k_x x + k_y y - \omega t)}\ e^{-\frac{k_x}{\omega}\int_0^x d(s)ds}\ ,$$

*and satisfies :*

- *$u \equiv v$ in the left half-space $x \le 0$, which means that we have no reflection at the interface : the layer model is perfectly mached.*
- *$u$ is damped in the right half-space,*
- *the damping coefficient in the absorbing layer is*

$$\frac{\|u(x)\|}{\|v(x)\|} = e^{-\frac{k_x}{\omega}\int_0^x d(s)ds}\ .$$

**Remark 1** *Notice that the damping is exponentially decreasing and it depends on the direction of propagation of the wave. More precisely, it decreases very fast for a wave propagating normally to the interface and increases when the direction of propagation approaches the parallel to the interface.*

# 3 Pml model for elastodynamics

In this section we present the PML model for the continuous elastodynamic problem. As we have seen in section 2 we know how to construct a PML model for an evolution problem of the form (1). Thus, in order to apply the technique described in the previous section to elastodynamics we need to write the elastodynamic problem in the form of system (1). This can be easily done once we consider the mixed velocity-stress formulation for elastodynamics.

## 3.1 The elastodynamic problem

We consider the 2D elastodynamic problem written as a first order hyperbolic system, the so called velocity-stress system

$$
\begin{array}{lll}
\varrho \dfrac{\partial v}{\partial t} - \mathbf{div}\sigma & = & 0 \\
A \dfrac{\partial \sigma}{\partial t} - \varepsilon(v) & = & 0 \\
+ \text{ initial condition.} &&
\end{array}
\tag{12}
$$

We suppose as in the previous section that the initial condition is supported in $\mathbb{R}^2_-$. In (12) $v = (v_x, v_y)$ denotes the velocity, $\sigma$ the stress tensor and $\varrho = \varrho(x)$ the density. If $u = (u_x, u_y)$ is the displacement then

$$
v = \frac{\partial u}{\partial t} \ .
$$

We denote $\varepsilon(u)$ the deformation tensor, i.e.,

$$
\varepsilon_{ij}(u) = \frac{1}{2}\left( \frac{\partial u_i}{\partial x_j} + \frac{\partial u_j}{\partial x_i} \right) \ .
$$

The stress tensor is related to the deformation tensor by Hooke's law

$$
\sigma = \sigma(u)(x,t) = C(x)\varepsilon(u)(x,t) \ ,
$$

where $C(x)$ is a $4 \times 4$ positive tensor having the classical properties of symmetry [1]. In system (12) we used

$$
A = A(x) = C^{-1}(x) \ .
$$

Finally we identify the tensor $\sigma$ with the following vector (still denoted by $\sigma$)

$$
\sigma = [\sigma_1,\ \sigma_2,\ \sigma_3]^t,\ \sigma_1 = \sigma_{xx} \ ;\ \sigma_2 = \sigma_{yy} \ ;\ \sigma_3 = \sigma_{xy} \ .
$$

We can write (12) in the following matrix form

$$
\begin{array}{ll}
\varrho \dfrac{\partial v}{\partial t} = D^{\parallel} \dfrac{\partial \sigma}{\partial y} + D^{\perp} \dfrac{\partial \sigma}{\partial x} & \text{in } \Omega \\
A \dfrac{\partial \sigma}{\partial t} = E^{\parallel} \dfrac{\partial v}{\partial y} + E^{\perp} \dfrac{\partial v}{\partial x} & \text{in } \Omega \ ,
\end{array}
$$

with

$$
D^{\parallel} = \begin{bmatrix} 0 & 0 & 1 \\ 0 & 1 & 0 \end{bmatrix}, \quad D^{\perp} = \begin{bmatrix} 1 & 0 & 0 \\ 0 & 0 & 1 \end{bmatrix},
$$

$$
E^{\parallel} = \begin{bmatrix} 0 & 0 \\ 0 & 1 \\ \frac{1}{2} & 0 \end{bmatrix}, \qquad E^{\perp} = \begin{bmatrix} 1 & 0 \\ 0 & 0 \\ 0 & \frac{1}{2} \end{bmatrix} \ ,
$$

We can apply now the same technique as in section 2 and we get the following system in the Perfectly Matched Layer($x > 0$)

$$
\begin{aligned}
& v = v^{\parallel} + v^{\perp} \\
& \varrho \frac{\partial v^{\parallel}}{\partial t} = D^{\parallel} \frac{\partial \sigma}{\partial y} \\
& \varrho \frac{\partial v^{\perp}}{\partial t} + d(x) v^{\perp} = D^{\perp} \frac{\partial \sigma}{\partial x} \ ,
\end{aligned}
$$

and

$$
\begin{aligned}
& \sigma = \sigma^{\parallel} + \sigma^{\perp} \\
& A \frac{\partial \sigma^{\parallel}}{\partial t} = E^{\parallel} \frac{\partial v}{\partial y} \\
& A \frac{\partial \sigma^{\perp}}{\partial t} + d(x) A \sigma^{\perp} = E^{\perp} \frac{\partial v}{\partial x} \ ,
\end{aligned}
$$

where $d(x)$ denotes the damping factor. In an homogeneous, isotropic elastic medium, the matrix $C(x)$ depends on the Lamé coefficients ($\lambda,\ \mu$) of the medium. In this case system (12) can be written in the following form

$$
\begin{aligned}
& \varrho \frac{\partial v_x}{\partial t} = \frac{\partial \sigma_{xx}}{\partial x} + \frac{\partial \sigma_{xy}}{\partial y} \quad ; \quad \frac{\partial \sigma_{xx}}{\partial t} = (\lambda + 2\mu) \frac{\partial v_x}{\partial x} + \lambda \frac{\partial v_y}{\partial y} \\
& \varrho \frac{\partial v_y}{\partial t} = \frac{\partial \sigma_{xy}}{\partial x} + \frac{\partial \sigma_{yy}}{\partial y} \quad ; \quad \frac{\partial \sigma_{yy}}{\partial t} = (\lambda + 2\mu) \frac{\partial v_y}{\partial y} + \lambda \frac{\partial v_x}{\partial x} \\
& \qquad\qquad\qquad\quad ; \quad \frac{\partial \sigma_{xy}}{\partial t} = \mu \frac{\partial v_y}{\partial x} + \mu \frac{\partial v_x}{\partial y} \ ,
\end{aligned} \tag{13}
$$

and the PML model becomes

$$
\begin{aligned}
& v = v^{\parallel} + v^{\perp} && ; \quad \sigma = \sigma^{\parallel} + \sigma^{\perp} \\
& \varrho \left(\frac{\partial}{\partial t} + d(x)\right) v_x^{\perp} = \frac{\partial \sigma_{xx}}{\partial x} && ; \quad \varrho \frac{\partial v_x^{\parallel}}{\partial t} = \frac{\partial \sigma_{xy}}{\partial y} \\
& \varrho \left(\frac{\partial}{\partial t} + d(x)\right) v_y^{\perp} = \frac{\partial \sigma_{xy}}{\partial x} && ; \quad \varrho \frac{\partial v_y^{\parallel}}{\partial t} = \frac{\partial \sigma_{yy}}{\partial y} \\
& \left(\frac{\partial}{\partial t} + d(x)\right) \sigma_{xx}^{\perp} = (\lambda + 2\mu) \frac{\partial v_x}{\partial x} && ; \quad \frac{\partial \sigma_{xx}^{\parallel}}{\partial t} = \lambda \frac{\partial v_y}{\partial y} \\
& \left(\frac{\partial}{\partial t} + d(x)\right) \sigma_{yy}^{\perp} = \lambda \frac{\partial v_x}{\partial x} && ; \quad \frac{\partial \sigma_{yy}^{\parallel}}{\partial t} = (\lambda + 2\mu) \frac{\partial v_y}{\partial y} \\
& \left(\frac{\partial}{\partial t} + d(x)\right) \sigma_{xy}^{\perp} = \mu \frac{\partial v_y}{\partial x} && ; \quad \frac{\partial \sigma_{xy}^{\parallel}}{\partial t} = \mu \frac{\partial v_x}{\partial y} \ .
\end{aligned} \tag{14}
$$

## 3.2 Plane wave analysis

### 3.2.1 Infinite absorbing layer

In the case of a homogeneous, isotropic elastic medium, following the same technique as in section 2, we can show that the plane waves, $U_j,\ j = p,\ s$, solution of system (13) can be written in the following form

$$
\begin{aligned}
& U_p = A_p \vec{d}_p e^{i\omega V_p (t - \frac{\cos(\theta) x + \sin(\theta) y}{V_p})} && \text{Pressure wave} \\
& U_s = A_s \vec{d}_s e^{i\omega V_s (t - \frac{-\sin(\theta) x + \cos(\theta) y}{V_s})} && \text{Shear wave} \ ,
\end{aligned} \tag{15}
$$

where $V_p = \sqrt{(\lambda + 2\mu)/\varrho}$ is the Pressure waves velocity, $V_s = \sqrt{\mu/\varrho}$ is the Shear waves velocity, $\theta$ gives the direction of wave propagation, $\vec{d}_j,\ j = p,\ s$ defines the direction of particle motion and $A_j,\ j = p,\ s$ is the amplitude of the waves. We can remark then that the plane waves, $\widetilde{U}_j,\ j = p,\ s$, solutions of system (14) can be written as

$$
\begin{aligned}
& \widetilde{U}_p = A_p \vec{d}_p e^{i\omega V_p (t - \frac{\cos(\theta) \tilde{x}_p + \sin(\theta) y}{V_p})} && \text{Pressure wave} \\
& \widetilde{U}_s = A_s \vec{d}_s e^{i\omega V_s (t - \frac{-\sin(\theta) \tilde{x}_s + \cos(\theta) y}{V_s})} && \text{Shear wave} \ ,
\end{aligned} \tag{16}
$$

where we simply substituted $x$ by $\tilde{x}_j,\ j = p,\ s$ in (15) and where $\tilde{x}_j,\ j = p,\ s$ is defined in the same way as in section 2 ($\omega$ replaced by $\omega V_j$)

$$\tilde{x}_j(x) = x - \frac{i}{\omega V_j}\int_0^x d(s)ds, \quad j = p,\ s\ .$$

Moreover we can show that $\widetilde{U}_j, j = p, s$ satisfy :

- $\widetilde{U}_j \equiv U_j,$ for $j = p,\ s$ in the left half-space $x \leq 0$ (no reflection),
- $\widetilde{U}_j, \quad j = p,\ s$ are damped in the right half-space,
- the damping coefficient in the absorbing layer is

$$\frac{\|\widetilde{U}_p(x)\|}{\|U_p(x)\|} = e^{-\frac{\cos\theta}{V_p}\int_0^x d(s)ds},$$
$$\frac{\|\widetilde{U}_s(x)\|}{\|U_s(x)\|} = e^{-\frac{\cos\theta}{V_s}\int_0^x d(s)ds}\ .$$

### 3.2.2 Finite absorbing layer

In practice, we take a finite absorbing layer by introducing a boundary at $x = \delta$, with a Dirichlet condition as we can see in Figure 2.

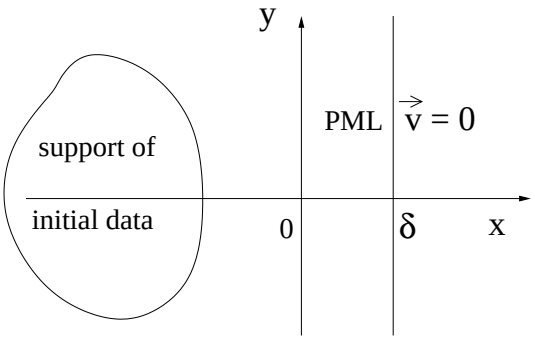


Figure 2: A finite PML layer.

This new boundary produces a reflection, but since the wave decreases exponentially in the layer, the reflection coefficient becomes quickly very small. This coefficient depends on the choice of $d(x)$ and on the size $\delta$ of the layer. In order to study the PML layer properties in this case, we recall some classical results for the elastodynamic problem.

Consider the elastodynamic problem with a homogeneous Dirichlet condition($\vec{v} = 0$) on the boundary $x = 0$ as shown in Figure 3. Take for example the case of an incident plane wave P

$$U_p^{inc} = A_{inc}\vec{d}_p e^{i\omega V_p(t - \frac{\vec{d}_p\cdot\vec{x}}{V_p})},\ \vec{d}_p = (\cos\theta, \sin\theta)\ .$$

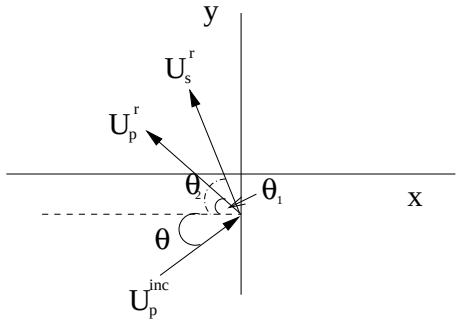


Figure 3: Reflection of an incident P wave.

We know then (c.f [1]) that the incident wave is reflected into a pressure wave $U_p^r$ and a shear wave $U_s^r$ given by

$$U_p^r = A_p^r \vec{d}_p^r e^{i\omega V_p (t - \frac{\vec{d}_p^r \cdot \vec{x}}{V_p})}, \quad \vec{d}_p^r = (-\cos\theta_1, \sin\theta_1)$$
$$U_s^r = A_s^r \vec{d}_s^r e^{i\omega V_p (t - \frac{\vec{p}_s \cdot \vec{x}}{V_p})}, \quad \vec{d}_s^r = (-\sin\theta_2, \cos\theta_2),$$
$$\vec{p}_s = (\cos\theta_2, \sin\theta_2) \ ,$$

and we have the reflection coefficients

$$R_{pp} = \frac{\|U_p^r\|}{\|U_p^{inc}\|} = \frac{\cos(\theta - \theta_2)}{\cos(\theta + \theta_2)}$$
$$R_{ps} = \frac{\|U_s^r\|}{\|U_p^{inc}\|} = \frac{\sin\theta_2}{\cos(\theta + \theta_2)}$$
$$\text{with } \sin\theta_2 = V_s \ \sin\theta / V_p \ .$$

In the same way in the case of an incident plane wave S we have

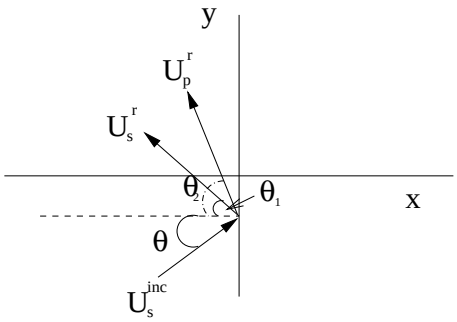


Figure 4: Reflection of an incident S wave.

$$R_{ss} = \frac{\|U_s^r\|}{\|U_s^{inc}\|} = \frac{\sin(\theta + \theta_2)}{\sin(\theta - \theta_2)}$$
$$R_{sp} = \frac{\|U_p^r\|}{\|U_s^{inc}\|} = \frac{\sin\theta_2}{\sin(\theta - \theta_2)}$$
$$\text{with } \cos\theta_2 = V_p \ \cos\theta / V_s \ .$$

We can consider now the case of the finite PML layer. Given that the plane waves, $U_j$, $j = p,\ s$, solution of system (13) are given by equations (15) we can compute the reflection coefficients induced by the PML layer of length $\delta$.

**The case of a plane wave P**

As we have shown previously there is no reflection at the interface $x = 0$ when the plane wave $\widetilde{U}_p$ penetrates

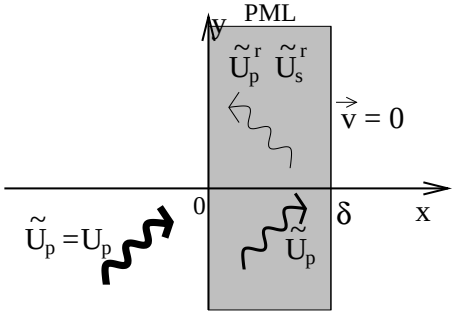


Figure 5: A plane wave P

the lossy medium. After traveling a length $\delta$ we can compute $\widetilde{U}_p$ using the formula (16), obtaining

$$\widetilde{U}_p = U_p e^{-\frac{\cos\theta}{V_p} \int_0^\delta d(s) ds} \ .$$

Then the plane wave $\widetilde{U}_p$, gives at the boundary $x = \delta$, two reflected waves $\widetilde{U}_p^r$ and $\widetilde{U}_s^r$, which are damped till penetrating again the elastic medium at the interface $x = 0$. It is easy to see that the reflection coefficient is given in this case by

$$
\begin{aligned}
R_{pp}^{\delta} &= \frac{\|\widetilde{U}_p^r(x)\|}{\|U_p(x)\|} = R_{pp} e^{-2\frac{\cos\theta}{V_p}\int_0^{\delta} d(s)ds}, \ x < 0 \\
R_{ps}^{\delta} &= \frac{\|\widetilde{U}_s^r(x)\|}{\|U_p(x)\|} = R_{ps} e^{-2\frac{\cos\theta}{V_p}\int_0^{\delta} d(s)ds}, \ x < 0 \ .
\end{aligned} \tag{17}
$$

**The case of a plane wave S**
In the case of an incident plane wave S, we obtain similarly

$$
\begin{aligned}
R_{ss}^{\delta} &= \frac{\|\widetilde{U}_s^r(x)\|}{\|U_s(x)\|} = R_{ss} e^{-2\frac{\cos\theta}{V_s}\int_0^{\delta} d(s)ds}, \ x < 0 \\
R_{sp}^{\delta} &= \frac{\|\widetilde{U}_p^r(x)\|}{\|U_s(x)\|} = R_{sp} e^{-2\frac{\cos\theta}{V_s}\int_0^{\delta} d(s)ds}, \ x < 0 \ .
\end{aligned} \tag{18}
$$

**Remark 2** *Relations (17) and (18) imply that the reflection can be made as weak as desired by choosing the damping factor $d(x)$ large enough. However this is no longer true when we consider the discrete PML model. As we will see in the next section, the discrete absorbing layer model is not perfectly matched. That is a consequence of the numerical dispersion, which introduces a reflection at the interface.*

# 4 The discrete PML model

In this section we present the discrete PML model for elastodynamics. To do so we introduce two numerical schemes for the discretization of system (12). The first one is a finite-differences scheme, introduced by Virieux in [22] and the second one is obtained using a new mixed finite element [3] in a regular mesh. The use of this finite element has the main advantage of leading to an explicit scheme (mass lumping), even in the case of an anisotropic elastic medium.

## 4.1 The Virieux finite-differences scheme

This scheme uses a staggered grid formulation, so that, if $v_x$ is computed at the points $(i,j)$ $(x_i = ih, y_j = jh)$ of a reference grid, then $v_y$ is computed at the points $(i+\frac{1}{2}, j+\frac{1}{2})$, $\sigma_{xx}$ and $\sigma_{yy}$ at $(i+\frac{1}{2}, j)$ and $\sigma_{xy}$ at $(i, j+\frac{1}{2})$. The disrcete PML model associated to the Virieux finite-differences scheme can be written as follows

$$
\begin{aligned}
&(v_x)_{i,j}^n = (v_x^x)_{i,j}^n + (v_x^y)_{i,j}^n \\
&\frac{(v_x^x)_{i,j}^{n+1} - (v_x^x)_{i,j}^n}{\Delta t} + d_i^x \frac{(v_x^x)_{i,j}^{n+1} + (v_x^x)_{i,j}^n}{2} = \frac{(\sigma_{xx})_{i^{\frac{1}{2}},j}^{n+\frac{1}{2}} - (\sigma_{xx})_{i^{-\frac{1}{2}},j}^{n+\frac{1}{2}}}{\varrho h} \\
&\frac{(v_x^y)_{i,j}^{n+1} - (v_x^y)_{i,j}^n}{\Delta t} + d_j^y \frac{(v_x^y)_{i,j}^{n+1} + (v_x^y)_{i,j}^n}{2} = \frac{(\sigma_{xy})_{i,j^{\frac{1}{2}}}^{n+\frac{1}{2}} - (\sigma_{xy})_{i,j^{-\frac{1}{2}}}^{n+\frac{1}{2}}}{\varrho h} \ ,
\end{aligned}
$$

$$
\begin{aligned}
&(v_y)_{i^{\frac{1}{2}},j^{\frac{1}{2}}}^n = (v_y^x)_{i^{\frac{1}{2}},j^{\frac{1}{2}}}^n + (v_y^y)_{i^{\frac{1}{2}},j^{\frac{1}{2}}}^n \\
&\frac{(v_y^x)_{i^{\frac{1}{2}},j^{\frac{1}{2}}}^{n+1} - (v_y^x)_{i^{\frac{1}{2}},j^{\frac{1}{2}}}^n}{\Delta t} + d_{i^{\frac{1}{2}}}^x \frac{(v_y^x)_{i^{\frac{1}{2}},j^{\frac{1}{2}}}^{n+1} + (v_y^x)_{i^{\frac{1}{2}},j^{\frac{1}{2}}}^n}{2} = \frac{(\sigma_{xy})_{i^1,j^{\frac{1}{2}}}^{n+\frac{1}{2}} - (\sigma_{xy})_{i,j^{\frac{1}{2}}}^{n+\frac{1}{2}}}{\varrho h} \\
&\frac{(v_y^y)_{i^{\frac{1}{2}},j^{\frac{1}{2}}}^{n+1} - (v_y^y)_{i^{\frac{1}{2}},j^{\frac{1}{2}}}^n}{\Delta t} + d_{j^{\frac{1}{2}}}^y \frac{(v_y^y)_{i^{\frac{1}{2}},j^{\frac{1}{2}}}^{n+1} + (v_y^y)_{i^{\frac{1}{2}},j^{\frac{1}{2}}}^n}{2} = \frac{(\sigma_{yy})_{i^{\frac{1}{2}},j^1}^{n+\frac{1}{2}} - (\sigma_{xy})_{i^{\frac{1}{2}},j}^{n+\frac{1}{2}}}{\varrho h} \ ,
\end{aligned}
$$

$$
\begin{aligned}
&(\sigma_{xx})^{n+\frac12}_{i\frac12,j} = (\sigma^x_{xx})^{n+\frac12}_{i\frac12,j} + (\sigma^y_{xx})^{n+\frac12}_{i\frac12,j}\\
&\frac{(\sigma^x_{xx})^{n+\frac12}_{i\frac12,j} - (\sigma^x_{xx})^{n-\frac12}_{i\frac12,j}}{\Delta t} + d^x_{i\frac12}\frac{(\sigma^x_{xx})^{n+\frac12}_{i\frac12,j} + (\sigma^x_{xx})^{n-\frac12}_{i\frac12,j}}{2} = (\lambda+2\mu)\frac{(v_x)^n_{i^1,j} - (v_x)^n_{i,j}}{h}\\
&\frac{(\sigma^y_{xx})^{n+\frac12}_{i\frac12,j} - (\sigma^y_{xx})^{n-\frac12}_{i\frac12,j}}{\Delta t} + d^y_{j}\frac{(\sigma^y_{xx})^{n+\frac12}_{i\frac12,j} + (\sigma^y_{xx})^{n-\frac12}_{i\frac12,j}}{2} = \lambda\frac{(v_y)^n_{i\frac12,j^{\frac12}} - (v_y)^n_{i\frac12,j^{-\frac12}}}{h},
\end{aligned}
$$

$$
\begin{aligned}
&(\sigma_{yy})^{n+\frac12}_{i\frac12,j} = (\sigma^x_{yy})^{n+\frac12}_{i\frac12,j} + (\sigma^y_{yy})^{n+\frac12}_{i\frac12,j}\\
&\frac{(\sigma^x_{yy})^{n+\frac12}_{i\frac12,j} - (\sigma^x_{yy})^{n-\frac12}_{i\frac12,j}}{\Delta t} + d^x_{i\frac12}\frac{(\sigma^x_{yy})^{n+\frac12}_{i\frac12,j} + (\sigma^x_{yy})^{n-\frac12}_{i\frac12,j}}{2} = \lambda\frac{(v_x)^n_{i^1,j} - (v_x)^n_{i,j}}{h}\\
&\frac{(\sigma^y_{yy})^{n+\frac12}_{i\frac12,j} - (\sigma^y_{yy})^{n-\frac12}_{i\frac12,j}}{\Delta t} + d^y_{j}\frac{(\sigma^y_{yy})^{n+\frac12}_{i\frac12,j} + (\sigma^y_{yy})^{n-\frac12}_{i\frac12,j}}{2} = (\lambda+2\mu)\frac{(v_y)^n_{i\frac12,j^{\frac12}} - (v_y)^n_{i\frac12,j^{-\frac12}}}{h},
\end{aligned}
$$

$$
\begin{aligned}
&(\sigma_{xy})^{n+\frac12}_{i,j\frac12} = (\sigma^x_{xy})^{n+\frac12}_{i,j\frac12} + (\sigma^y_{xy})^{n+\frac12}_{i,j\frac12}\\
&\frac{(\sigma^x_{xy})^{n+\frac12}_{i,j\frac12} - (\sigma^x_{xy})^{n-\frac12}_{i,j\frac12}}{\Delta t} + d^x_{i}\frac{(\sigma^x_{xy})^{n+\frac12}_{i,j\frac12} + (\sigma^x_{xy})^{n-\frac12}_{i,j\frac12}}{2} = \mu\frac{(v_y)^n_{i^{\frac12},j^{\frac12}} - (v_y)^n_{i^{-\frac12},j^{\frac12}}}{h}\\
&\frac{(\sigma^y_{xy})^{n+\frac12}_{i,j\frac12} - (\sigma^y_{xy})^{n-\frac12}_{i,j\frac12}}{\Delta t} + d^y_{j\frac12}\frac{(\sigma^y_{xy})^{n+\frac12}_{i,j\frac12} + (\sigma^y_{xy})^{n-\frac12}_{i,j\frac12}}{2} = \mu\frac{(v_x)^n_{i,j^1} - (v_x)^n_{i,j}}{h}.
\end{aligned}
$$

where we used the notation $i^k = i + k$ and $j^k = j + k$.
The previous system of equations corresponds to the PML model in the corners, where we need a damping in both directions. For the computation of the solution inside the PML layers in the $x$ direction we use the same system of equations with $d^y = 0$, while for PML layers in the $y$ direction we take $d^x = 0$. We present in Figure 6 the values of $d^x$ and $d^y$ for the different PML layers.

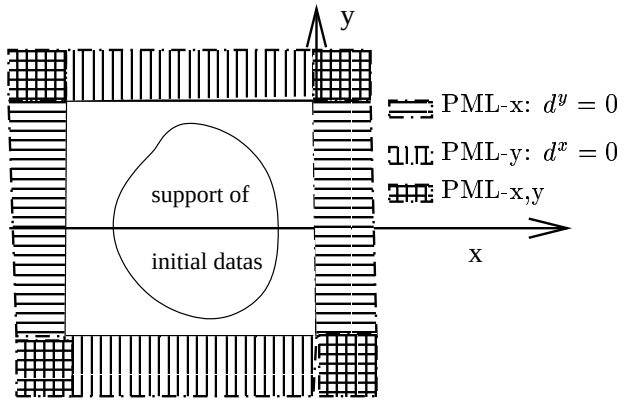


Figure 6: PML layers.

## 4.2 The finite-element scheme

For this scheme, the velocity is approximated by piecewise constant functions and the stress tensor $\sigma$ by $Q_1$ functions with some particular continuity properties :

- $\sigma_{xy}$ is continuous in both directions : it is approximated by $Q_1$ continuous functions.
- $\sigma_{xx}$ is continuous only in the $x$ direction : it is approximated by $Q_1$ functions continuous in $x$ and discontinuous in $y$ direction.

- $\sigma_{yy}$ is continuous only in the $y$ direction : it is approximated by $Q_1$ functions continuous in $y$ and discontinuous in $x$ direction.

We present in Figure 7 the mixed finite element used.

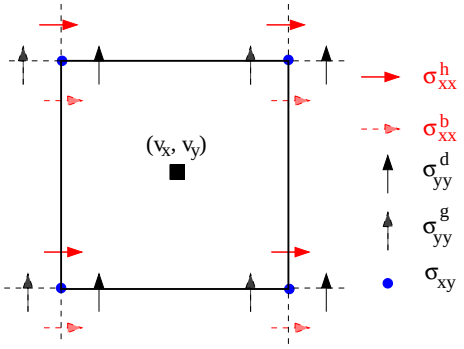


Figure 7: The finite element

On a regular grid, the velocity $v = (v_x, v_y)$ is computed at the points $(i^{\frac{1}{2}}, j^{\frac{1}{2}})$ and the stress tensor at the points $(i, j)$. We consider the general case of an anisotropic elastic material described by the elasticity matrix $C$, and we denote by $A$ the inverse of C

$$A = C^{-1} = \begin{bmatrix} a_{11} & a_{12} & a_{13} \\ a_{12} & a_{22} & a_{23} \\ a_{13} & a_{23} & a_{33} \end{bmatrix}$$

The numerical scheme can then be written in the following way (see [4] for details). For the first equation of system (12) we have

$$\frac{(v_x)^{n+1}_{i^{\frac{1}{2}},j^{\frac{1}{2}}} - (v_x)^{n}_{i^{\frac{1}{2}},j^{\frac{1}{2}}}}{\Delta t} = \frac{1}{2\varrho h}\Big((\sigma^h_{xx})^{n+\frac{1}{2}}_{i^1,j} - (\sigma^h_{xx})^{n+\frac{1}{2}}_{i,j} + (\sigma^b_{xx})^{n+\frac{1}{2}}_{i^1,j^1} - (\sigma^b_{xx})^{n+\frac{1}{2}}_{i,j^1} + (\sigma_{xy})^{n+\frac{1}{2}}_{i,j^1} - (\sigma_{xy})^{n+\frac{1}{2}}_{i,j} + (\sigma_{xy})^{n+\frac{1}{2}}_{i^1,j^1} - (\sigma_{xy})^{n+\frac{1}{2}}_{i^1,j}\Big)$$

$$\frac{(v_y)^{n+1}_{i^{\frac{1}{2}},j^{\frac{1}{2}}} - (v_y)^{n}_{i^{\frac{1}{2}},j^{\frac{1}{2}}}}{\Delta t} = \frac{1}{2\varrho h}\Big((\sigma_{xy})^{n+\frac{1}{2}}_{i^1,j} - (\sigma_{xy})^{n+\frac{1}{2}}_{i,j} + (\sigma_{xy})^{n+\frac{1}{2}}_{i^1,j^1} - (\sigma_{xy})^{n+\frac{1}{2}}_{i,j^1} + (\sigma^d_{yy})^{n+\frac{1}{2}}_{i,j^1} - (\sigma^d_{yy})^{n+\frac{1}{2}}_{i,j} + (\sigma^g_{yy})^{n+\frac{1}{2}}_{i^1,j^1} - (\sigma^g_{yy})^{n+\frac{1}{2}}_{i^1,j}\Big)$$

The second equation of system (12) results in the following $5 \times 5$ local system, coupling the five degrees of freedom associated to $\sigma$ at each vertex (see Figure 7).

$$\frac{\Sigma^{n+\frac{1}{2}}_{i,j} - \Sigma^{n-\frac{1}{2}}_{i,j}}{\Delta t} = A_h^{-1} B_h^x + A_h^{-1} B_h^y$$

where

$$\Sigma = \left[\sigma^h_{xx},\ \sigma^b_{xx},\ \sigma^d_{yy},\ \sigma^g_{yy}, \sigma_{xy}\right]^t$$

$$A_h = \frac{1}{2}\begin{bmatrix} 2a_{11} & 0 & a_{12} & a_{12} & 2a_{13} \\ 0 & 2a_{11} & a_{12} & a_{12} & 2a_{13} \\ a_{12} & a_{12} & 2a_{22} & 0 & 2a_{23} \\ a_{12} & a_{12} & 0 & 2a_{22} & 2a_{23} \\ 2a_{13} & 2a_{13} & 2a_{23} & 2a_{23} & 4a_{33} \end{bmatrix}$$

and

$$B_h^x = \frac{1}{h}\,[B_1^x,\ B_2^x,\ 0,\ 0,\ B_5^x]^t$$

$$B_h^y = \frac{1}{h}\,[0,\ 0,\ B_3^y,\ B_4^y,\ B_5^y]^t$$

with

$$\begin{aligned}
B_1^x &= (v_x)^n_{i^{\frac12},j^{\frac12}} - (v_x)^n_{i^{-\frac12},j^{\frac12}}\\
B_2^x &= (v_x)^n_{i^{\frac12},j^{-\frac12}} - (v_x)^n_{i^{-\frac12},j^{-\frac12}}\\
B_3^y &= (v_y)^n_{i^{\frac12},j^{\frac12}} - (v_y)^n_{i^{\frac12},j^{-\frac12}}\\
B_4^y &= (v_y)^n_{i^{-\frac12},j^{\frac12}} - (v_y)^n_{i^{-\frac12},j^{-\frac12}}\\
B_5^x &= (v_y)^n_{i^{\frac12},j^{\frac12}} - (v_y)^n_{i^{-\frac12},j^{\frac12}} + (v_y)^n_{i^{\frac12},j^{-\frac12}} - (v_y)^n_{i^{-\frac12},j^{-\frac12}}\\
B_5^y &= (v_x)^n_{i^{\frac12},j^{\frac12}} - (v_x)^n_{i^{\frac12},j^{-\frac12}} + (v_x)^n_{i^{-\frac12},j^{\frac12}} - (v_x)^n_{i^{-\frac12},j^{-\frac12}}
\end{aligned}$$

In the case of an isotropic elastic material the matrix $A_h^{-1}$ is given by

$$A_h^{-1} = \begin{bmatrix} a & c & b & b & 0\\ c & a & b & b & 0\\ b & b & a & c & 0\\ b & b & c & a & 0\\ 0 & 0 & 0 & 0 & d \end{bmatrix}$$

with

$$a = \frac{2(\lambda+2\mu)^2-\lambda^2}{2(\lambda+2\mu)},\quad b = \frac{\lambda}{2},\quad c = \frac{\lambda^2}{2(\lambda+2\mu)},\ d = \frac{\mu}{2}\ . \tag{19}$$

We can write now the PML model associated to this scheme, using the same technique as for the Virieux scheme

$$\begin{aligned}
&(v_x)^n_{i^{\frac12},j^{\frac12}} = (v_x^x)^n_{i^{\frac12},j^{\frac12}} + (v_x^y)^n_{i^{\frac12},j^{\frac12}}\\
&\frac{(v_x^x)^{n+1}_{i^{\frac12},j^{\frac12}} - (v_x^x)^n_{i^{\frac12},j^{\frac12}}}{\Delta t} + d^x_{i^{\frac12}}\frac{(v_x^x)^{n+1}_{i^{\frac12},j^{\frac12}} + (v_x^x)^n_{i^{\frac12},j^{\frac12}}}{2} = \frac{1}{2\varrho h}\left((\sigma^h_{xx})^{n+\frac12}_{i^1,j} - (\sigma^h_{xx})^{n+\frac12}_{i,j} + (\sigma^b_{xx})^{n+\frac12}_{i^1,j^1} - (\sigma^b_{xx})^{n+\frac12}_{i,j^1}\right)\\
&\frac{(v_x^y)^{n+1}_{i^{\frac12},j^{\frac12}} - (v_x^y)^n_{i^{\frac12},j^{\frac12}}}{\Delta t} + d^y_{i^{\frac12}}\frac{(v_x^y)^{n+1}_{i^{\frac12},j^{\frac12}} + (v_x^y)^n_{i^{\frac12},j^{\frac12}}}{2} = \frac{1}{2\varrho h}\left((\sigma_{xy})^{n+\frac12}_{i,j^1} - (\sigma_{xy})^{n+\frac12}_{i,j} + (\sigma_{xy})^{n+\frac12}_{i^1,j^1} - (\sigma_{xy})^{n+\frac12}_{i^1,j}\right)
\end{aligned}$$

$$\begin{aligned}
&(v_y)^n_{i^{\frac12},j^{\frac12}} = (v_y^x)^n_{i^{\frac12},j^{\frac12}} + (v_y^y)^n_{i^{\frac12},j^{\frac12}}\\
&\frac{(v_y^x)^{n+1}_{i^{\frac12},j^{\frac12}} - (v_y^x)^n_{i^{\frac12},j^{\frac12}}}{\Delta t} + d^x_{i^{\frac12}}\frac{(v_y^x)^{n+1}_{i^{\frac12},j^{\frac12}} + (v_y^x)^n_{i^{\frac12},j^{\frac12}}}{2} = \frac{1}{2\varrho h}\left((\sigma_{xy})^{n+\frac12}_{i^1,j} - (\sigma_{xy})^{n+\frac12}_{i,j} + (\sigma_{xy})^{n+\frac12}_{i^1,j^1} - (\sigma_{xy})^{n+\frac12}_{i,j^1}\right)\\
&\frac{(v_y^y)^{n+1}_{i^{\frac12},j^{\frac12}} - (v_y^y)^n_{i^{\frac12},j^{\frac12}}}{\Delta t} + d^y_{i^{\frac12}}\frac{(v_y^y)^{n+1}_{i^{\frac12},j^{\frac12}} + (v_y^y)^n_{i^{\frac12},j^{\frac12}}}{2} = \frac{1}{2\varrho h}\left((\sigma^d_{yy})^{n+\frac12}_{i,j^1} - (\sigma^d_{yy})^{n+\frac12}_{i,j} + (\sigma^g_{yy})^{n+\frac12}_{i^1,j^1} - (\sigma^g_{yy})^{n+\frac12}_{i^1,j}\right)
\end{aligned}$$

and

$$\begin{aligned}
&\Sigma^{n+\frac12}_{i,j} = (\Sigma^x)^{n+\frac12}_{i,j} + (\Sigma^y)^{n+\frac12}_{i,j}\\
&\frac{(\Sigma^x)^{n+\frac12}_{i,j} - (\Sigma^x)^{n-\frac12}_{i,j}}{\Delta t} + d^x_i\frac{(\Sigma^x)^{n+\frac12}_{i,j} + (\Sigma^x)^{n-\frac12}_{i,j}}{2} = M_h^{-1}B_h^x\\
&\frac{(\Sigma^y)^{n+\frac12}_{i,j} - (\Sigma^y)^{n-\frac12}_{i,j}}{\Delta t} + d^y_i\frac{(\Sigma^y)^{n+\frac12}_{i,j} + (\Sigma^y)^{n-\frac12}_{i,j}}{2} = M_h^{-1}B_h^y
\end{aligned}$$

# 5 Dispersion Analysis

In this section we will study the properties of the discrete PML model for elastodynamics in terms of a numerical dispersion analysis, that is a plane wave analysis. We present this analysis only for the finite-element scheme. We consider the case of an homogeneous isotropic elastic medium characterized by the Lamé coefficients $\lambda$, $\mu$ and the density $\varrho$. The PML layer is in the $x-direction$ (Figure 1) and we consider the case of a infinite layer. We look for plane wave solutions of the form

$$
\begin{aligned}
(v_x^l)^{n+\frac{1}{2}}_{i^{\frac{1}{2}},j^{\frac{1}{2}}} &= (\hat{v}_x^l)_{i^{\frac{1}{2}}} e^{-ik_y(j^{\frac{1}{2}})h+i\omega(n+\frac{1}{2})\Delta t}, \quad l=\perp,\ \| \\
(v_y^l)^{n+\frac{1}{2}}_{i^{\frac{1}{2}},j^{\frac{1}{2}}} &= (\hat{v}_y^l)_{i^{\frac{1}{2}}} e^{-ik_y(j^{\frac{1}{2}})h+i\omega(n+\frac{1}{2})\Delta t}, \quad l=\perp,\ \| \\
(\sigma_{xx}^{h,l})^n_{i,j} &= (\hat{\sigma}_{xx}^{h,l})_i e^{-ik_y jh+i\omega n\Delta t}, \quad l=\perp,\ \| \\
(\sigma_{xx}^{b,l})^n_{i,j} &= (\hat{\sigma}_{xx}^{b,l})_i e^{-ik_y jh+i\omega n\Delta t}, \quad l=\perp,\ \| \\
(\sigma_{yy}^{d,l})^n_{i,j} &= (\hat{\sigma}_{yy}^{d,l})_i e^{-ik_y jh+i\omega n\Delta t}, \quad l=\perp,\ \| \\
(\sigma_{yy}^{g,l})^n_{i,j} &= (\hat{\sigma}_{yy}^{g,l})_i e^{-ik_y jh+i\omega n\Delta t}, \quad l=\perp,\ \| \\
(\sigma_{xy}^{l})^n_{i,j} &= (\hat{\sigma}_{xy}^{l})_i e^{-ik_y jh+i\omega n\Delta t}, \quad l=\perp,\ \|
\end{aligned}
$$

and we set

$$
\begin{aligned}
&(\hat{v}_x)_{i^{\frac{1}{2}}} = (\hat{v}_x^{\|})_{i^{\frac{1}{2}}} + (\hat{v}_x^{\perp})_{i^{\frac{1}{2}}} \quad ; \quad (\hat{v}_y)_{i^{\frac{1}{2}}} = (\hat{v}_y^{\|})_{i^{\frac{1}{2}}} + (\hat{v}_y^{\perp})_{i^{\frac{1}{2}}} \\
&(\hat{\sigma}_{xx}^{h})_i = (\hat{\sigma}_{xx}^{h,\|})_i + (\hat{\sigma}_{xx}^{h,\perp})_i \quad ; \quad (\hat{\sigma}_{xx}^{b})_i = (\hat{\sigma}_{xx}^{b,\|})_i + (\hat{\sigma}_{xx}^{b,\perp})_i \\
&(\hat{\sigma}_{yy}^{d})_i = (\hat{\sigma}_{yy}^{d,\|})_i + (\hat{\sigma}_{yy}^{d,\perp})_i \quad ; \quad (\hat{\sigma}_{yy}^{g})_i = (\hat{\sigma}_{yy}^{g,\|})_i + (\hat{\sigma}_{yy}^{g,\perp})_i \\
&(\hat{\sigma}_{xy})_i = (\hat{\sigma}_{xy}^{\|})_i + (\hat{\sigma}_{xy}^{\perp})_i \ .
\end{aligned}
$$

Plugging these expression into the discrete scheme, gives

$$
\begin{aligned}
\frac{A_t}{\Delta t}(\hat{v}_x^{\|})_{i^{\frac{1}{2}}} &= -Ay\frac{(\hat{\sigma}_{xy})_{i^1} + (\hat{\sigma}_{xy})_i}{2\varrho h} \\
\frac{C_{i^{\frac{1}{2}}}}{\Delta t}(\hat{v}_x^{\perp})_{i^{\frac{1}{2}}} &= e^{ik_y h/2}\frac{(\hat{\sigma}_{xx}^{h})_{i^1} - (\hat{\sigma}_{xx}^{h})_i}{2\varrho h} \\
&\quad + e^{-ik_y h/2}\frac{(\hat{\sigma}_{xx}^{b})_{i^1} - (\hat{\sigma}_{xx}^{b})_i}{2\varrho h} \\
\frac{A_t}{\Delta t}(\hat{v}_y^{\|})_{i^{\frac{1}{2}}} &= -Ay\frac{(\hat{\sigma}_{yy}^{g})_{i^1} + (\hat{\sigma}_{yy}^{d})_i}{2\varrho h} \\
\frac{C_{i^{\frac{1}{2}}}}{\Delta t}(\hat{v}_x^{\perp})_{i^{\frac{1}{2}}} &= \cos\left(\frac{k_y h}{2}\right)\frac{(\hat{\sigma}_{xy})_{i^1} - (\hat{\sigma}_{xy})_i}{\varrho h} \ ,
\end{aligned}
$$

$$
\begin{aligned}
\frac{A_t}{\Delta t}(\hat{\sigma}_{xy}^{\|})_i &= -\mu Ay\frac{(\hat{v}_x)_{i^{\frac{1}{2}}} + (\hat{v}_x)_{i^{-\frac{1}{2}}}}{2h} \\
\frac{C_i}{\Delta t}(\hat{\sigma}_{xy}^{\perp})_i &= \mu\cos\left(\frac{k_y h}{2}\right)\frac{(\hat{v}_y)_{i^{\frac{1}{2}}} - (\hat{v}_y)_{i^{-\frac{1}{2}}}}{h} \ ,
\end{aligned}
$$

$$
\begin{aligned}
\frac{A_t}{\Delta t}(\hat{\sigma}_{xx}^{h,\|})_i &= -bAy\frac{(\hat{v}_y)_{i^{\frac{1}{2}}} + (\hat{v}_y)_{i^{-\frac{1}{2}}}}{h} \\
\frac{C_i}{\Delta t}(\hat{\sigma}_{xx}^{h,\perp})_i &= \left(ae^{-ik_y h/2} + ce^{ik_y h/2}\right)\frac{(\hat{v}_x)_{i^{\frac{1}{2}}} - (\hat{v}_x)_{i^{-\frac{1}{2}}}}{h} \\
\frac{A_t}{\Delta t}(\hat{\sigma}_{xx}^{b,\|})_i &= -bAy\frac{(\hat{v}_y)_{i^{\frac{1}{2}}} + (\hat{v}_y)_{i^{-\frac{1}{2}}}}{h} \\
\frac{C_i}{\Delta t}(\hat{\sigma}_{xx}^{b,\perp})_i &= \left(ae^{ik_y h/2} + ce^{-ik_y h/2}\right)\frac{(\hat{v}_x)_{i^{\frac{1}{2}}} - (\hat{v}_x)_{i^{-\frac{1}{2}}}}{h} \ ,
\end{aligned}
$$

and

$$\begin{aligned}
\frac{A_t}{\Delta t}(\hat{\sigma}^{d,\parallel}_{yy})_i &= -Ay\frac{a(\hat{v}_y)_{i^{\frac{1}{2}}} + c(\hat{v}_y)_{i^{-\frac{1}{2}}}}{h} \\
\frac{C_i}{\Delta t}(\hat{\sigma}^{d,\perp}_{yy})_i &= 2b\cos\left(\frac{k_y h}{2}\right)\frac{(\hat{v}_x)_{i^{\frac{1}{2}}} - (\hat{v}_x)_{i^{-\frac{1}{2}}}}{h} \\
\frac{A_t}{\Delta t}(\hat{\sigma}^{g,\parallel}_{yy})_i &= -Ay\frac{c(\hat{v}_y)_{i^{\frac{1}{2}}} + a(\hat{v}_y)_{i^{-\frac{1}{2}}}}{h} \\
\frac{C_i}{\Delta t}(\hat{\sigma}^{g,\perp}_{yy})_i &= 2b\cos\left(\frac{k_y h}{2}\right)\frac{(\hat{v}_x)_{i^{\frac{1}{2}}} - (\hat{v}_x)_{i^{-\frac{1}{2}}}}{h}\ ,
\end{aligned}$$

where $a,\ b,\ c$ are given by (19) and $A_t,\ A_y$ and $C_l$ are defined by

$$\begin{aligned}
A_t &= 2i\sin\left(\frac{\omega\Delta t}{2}\right),\ A_y = 2i\sin\left(\frac{k_y h}{2}\right) \\
C_l &= 2i\sin\left(\frac{\omega\Delta t}{2}\right) + d_l\ \Delta t\cos\left(\frac{\omega\Delta t}{2}\right),\ l = i, i^{\frac{1}{2}}\ .
\end{aligned}$$

After some tedious calculations, we can rewrite the previous system of equations with $\hat{v}_x,\ \hat{v}_y$ as the only unknowns. We obtain

$$\begin{aligned}
&\frac{A_t^2}{\Delta t^2}(\hat{v}_x)_{i^{\frac{1}{2}}} = \frac{\mu}{\varrho}A_y^2\frac{(\hat{v}_x)_{i^{\frac{3}{2}}} + 2(\hat{v}_x)_{i^{\frac{1}{2}}} + (\hat{v}_x)_{i^{-\frac{1}{2}}}}{4h^2} \\
&+\frac{a + c\cos(k_y h)}{\varrho D_{i^{\frac{1}{2}}}}\left(\frac{(\hat{v}_x)_{i^{\frac{3}{2}}} - (\hat{v}_x)_{i^{\frac{1}{2}}}}{h^2 D_{i^1}} - \frac{(\hat{v}_x)_{i^{\frac{1}{2}}} - (\hat{v}_x)_{i^{-\frac{1}{2}}}}{h^2 D_i}\right) \\
&-A_y\frac{\mu}{\varrho}\cos\left(\frac{k_y h}{2}\right)\left(\frac{(\hat{v}_y)_{i^{\frac{3}{2}}} - (\hat{v}_y)_{i^{\frac{1}{2}}}}{2h^2 D_{i^1}} + \frac{(\hat{v}_y)_{i^{\frac{1}{2}}} - (\hat{v}_y)_{i^{-\frac{1}{2}}}}{2h^2 D_i}\right. \\
&\qquad\left. +\frac{(\hat{v}_y)_{i^{\frac{3}{2}}} - (\hat{v}_y)_{i^{-\frac{1}{2}}}}{h^2 D_{i^{\frac{1}{2}}}}\right) \\
&\frac{A_t^2}{\Delta t^2}(\hat{v}_y)_{i^{\frac{1}{2}}} = \frac{1}{\varrho}A_y^2\frac{c(\hat{v}_y)_{i^{\frac{3}{2}}} + 2a(\hat{v}_y)_{i^{\frac{1}{2}}} + c(\hat{v}_y)_{i^{-\frac{1}{2}}}}{2h^2} \\
&+\frac{\mu}{\varrho}\cos^2\left(\frac{k_y h}{2}\right)\left(\frac{(\hat{v}_y)_{i^{\frac{3}{2}}} - (\hat{v}_y)_{i^{\frac{1}{2}}}}{h^2 D_{i^1} D_{i^{\frac{1}{2}}}} - \frac{(\hat{v}_y)_{i^{\frac{1}{2}}} - (\hat{v}_y)_{i^{-\frac{1}{2}}}}{h^2 D_i D_{i^{\frac{1}{2}}}}\right) \\
&-A_y\frac{b}{\varrho}\cos\left(\frac{k_y h}{2}\right)\left(\frac{(\hat{v}_x)_{i^{\frac{3}{2}}} - (\hat{v}_x)_{i^{\frac{1}{2}}}}{h^2 D_{i^1}} + \frac{(\hat{v}_x)_{i^{\frac{1}{2}}} - (\hat{v}_x)_{i^{-\frac{1}{2}}}}{h^2 D_i}\right. \\
&\qquad\left. +\frac{(\hat{v}_x)_{i^{\frac{3}{2}}} - (\hat{v}_x)_{i^{-\frac{1}{2}}}}{2h^2 D_{i^{\frac{1}{2}}}}\right)\ ,
\end{aligned} \tag{20}$$

with

$$D_l = \frac{C_l}{A_t}, l = i,\ i^{\frac{1}{2}}\ .$$

Let us consider now the case of a medium with a unique infinite layer for which

$$d_i = \begin{cases} 0 & \text{if } i \le 0 \\ d_\infty & \text{if } i > 0 \end{cases},\ d_{i^{\frac{1}{2}}} = \begin{cases} 0 & \text{if } i < 0 \\ d_\infty & \text{if } i > 0\ , \end{cases}$$

$d_{\frac{1}{2}}$ remaining undetermined yet, and let us look for particular solution of the form

$$
\begin{aligned}
&\textbf{P wave}\\
(\hat{V})_{i\frac{1}{2}} &= \vec{d_p} e^{-ik_x(i\frac{1}{2})h} + R_{pp}\vec{d_p^r} e^{ik_x(i\frac{1}{2})h}\\
&\quad + R_{ps}\vec{d_s^r} e^{ik_x(i\frac{1}{2})h} \text{ for } i\tfrac{1}{2} \leq 0\\
(\hat{V})_{i\frac{1}{2}} &= T_{pp}\widetilde{d}_p e^{-i\widetilde{k}_x(i\frac{1}{2})h} + T_{ps}\widetilde{d}_s e^{-i\widetilde{k}_x(i\frac{1}{2})h} \text{ for } i\tfrac{1}{2} \geq 0\\
&\textbf{S wave}\\
(\hat{V})_{i\frac{1}{2}} &= \vec{d_s} e^{-ik_x(i\frac{1}{2})h} + R_{ss}\vec{d_s^r} e^{ik_x(i\frac{1}{2})h}\\
&\quad + R_{sp}\vec{d_p^r} e^{ik_x(i\frac{1}{2})h} \text{ for } i + \frac{1}{2} \leq 0\\
(\hat{V})_{i\frac{1}{2}} &= T_{ss}\widetilde{d}_s e^{-i\widetilde{k}_x(i\frac{1}{2})h} + T_{sp}\widetilde{d}_p e^{-i\widetilde{k}_x(i\frac{1}{2})h} \text{ for } i\tfrac{1}{2} \geq 0\ ,
\end{aligned}
\tag{21}
$$

where

$$
(\hat{V})_{i\frac{1}{2}} = \begin{bmatrix} (\hat{v}_x)_{i\frac{1}{2}} \\ (\hat{v}_y)_{i\frac{1}{2}} \end{bmatrix} .
$$

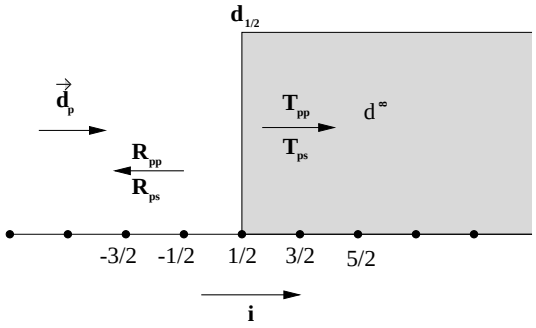


Figure 8: Schematic view on the plane waves solution in a single layer discrete model

The equations (20) are satisfied for $i\frac{1}{2} \neq 0$ if $k_x$ and $\widetilde{k}_x$ are solutions of the two relations of dispersion (22) (free medium) and (23) (lossy medium).

$$
\frac{X_t^2}{\Delta t^2}\begin{bmatrix} \hat{v}_x \\ \hat{v}_x \end{bmatrix} = \frac{1}{h^2}\begin{bmatrix} \hat{K}_{11} & \hat{K}_{12} \\ \hat{K}_{12} & \hat{K}_{22} \end{bmatrix}\begin{bmatrix} \hat{v}_x \\ \hat{v}_x \end{bmatrix} , \tag{22}
$$

$$
\frac{X_t^2}{\Delta t^2}\begin{bmatrix} \hat{v}_x \\ \hat{v}_x \end{bmatrix} = \frac{1}{h^2}\begin{bmatrix} \widetilde{K}_{11} & \widetilde{K}_{12} \\ \widetilde{K}_{12} & \widetilde{K}_{22} \end{bmatrix}\begin{bmatrix} \hat{v}_x \\ \hat{v}_x \end{bmatrix} , \tag{23}
$$

with

$$
\begin{aligned}
\hat{K}_{11} &= V_p^2 X_x(1 - 4\alpha X_y) + V_s^2 X_y(1 - \beta X_x)\\
\hat{K}_{22} &= V_p^2 X_y(1 - 4\alpha X_x) + V_s^2 X_x(1 - \beta X_y)\\
\hat{K}_{12} &= (V_p^2 - V_s^2)\sqrt{X_x X_y(1 - X_x)(1 - X_y)}
\end{aligned}
$$

$$
X_t = \sin^2\left(\frac{\omega\Delta t}{2}\right),\ X_x = \sin^2\left(\frac{k_x h}{2}\right)
$$

$$
X_y = \sin^2\left(\frac{k_y h}{2}\right),\ \alpha = \frac{(V_p^2 - 2V_s^2)^2}{4V_p^4},\ \beta = \frac{1}{4}
$$

and

$$\widetilde{K}_{11} = V_p^2 \frac{\widetilde{X}_x}{\widetilde{D}^2}(1-4\alpha X_y) + V_s^2 X_y (1-\beta \widetilde{X}_x)$$
$$\widetilde{K}_{22} = V_p^2 X_y (1-4\alpha \widetilde{X}_x) + V_s^2 \frac{\widetilde{X}_x}{\widetilde{D}^2}(1-\beta X_y)$$
$$\widetilde{K}_{12} = \frac{(V_p^2 - V_s^2)}{\widetilde{D}} \sqrt{\widetilde{X}_x X_y (1-\widetilde{X}_x)(1-X_y)}$$
$$\widetilde{X}_x = \sin^2\left(\frac{\widetilde{k}_x h}{2}\right),\ \widetilde{D} = \frac{2i\sin\left(\frac{\omega\Delta t}{2}\right) + d_\infty\ \Delta t \cos\left(\frac{\omega\Delta t}{2}\right)}{2i\sin\left(\frac{\omega\Delta t}{2}\right)}.$$

Now, the system of equations at $i\frac{1}{2} = 0$ gives the value of the reflection coefficients $R_{pp}$(resp. $R_{ss}$) and $R_{ps}$(resp. $R_{sp}$). We have used the software MAPLE to compute its Taylor expansion with respect to the discretization step and we obtain

$$\begin{aligned}
R_{pp} &= \frac{d_\infty - 2d_{\frac{1}{2}}}{4\omega}\left(1 - 2r_1^2(V_p^2+V_s^2)\right)\frac{r_0}{V_p}h + O(h^2)\\
R_{ps} &= \frac{d_\infty - 2d_{\frac{1}{2}}}{4\omega}\left(3 - 2r_1^2(V_p^2+V_s^2)\right)k_y h + O(h^2)\\
R_{ss} &= \frac{d_\infty - 2d_{\frac{1}{2}}}{4\omega}\left(1 - 2r_2^2 r_1^2(V_p^2+V_s^2)\right)\frac{r_0}{V_p}h + O(h^2)\\
R_{sp} &= \frac{d_\infty - 2d_{\frac{1}{2}}}{4\omega}\left(2r_2^2 r_1^2(V_p^2+V_s^2) - 1 - 2r_2^2\right)k_y h + O(h^2)
\end{aligned} \tag{24}$$

with

$$r_0 = \sqrt{\omega^2 - V_p^2 k_y^2},\ r_1 = \frac{k_y^2}{\omega^2},\ r_2 = \frac{V_s^2}{V_p^2},\ r_3 = \frac{1}{r_2}\ .$$

From relations (24), we can easily remark that the best choice for $d_{\frac{1}{2}}$ consists in taking

$$d_{\frac{1}{2}} = \frac{d_\infty}{2}\ .$$

In that case, the first order terms in (24) disappear and we obtain that the reflection coefficients are roughly proportional to $d_\infty(d_\infty + i\omega)h^2$. Two consequences can be deduced from this result. First the numerical scheme is consistent with the continuous PML model : the spurious reflection for a given value of $d_\infty$ is only due to the dispersion of the numerical scheme. Let us remark that the second order accuracy is recovered in the $h^2$ dependency of the reflection coefficients. Then, from a more practical point of view, this dispersion analysis implies that we can not use a value of $d_\infty$ too large for a given discretization step.

In the case of a finite length layer with a given number of nodes, the layer is characterized by

$$\begin{cases} (d_{\frac{1}{2}},\ d_{\frac{3}{2}},\ ...,d_{n_l-\frac{1}{2}}),\\ (d_1,\ d_2,\ ...,d_{n_l}), \end{cases}$$

we are then led to find a trade off between choosing the $d_{i+\frac{1}{2}}$'s too weak (which would imply a strong reflection due to the Dirichlet boundary condition) or too large (which would imply spurious reflections due to the dispersion). A partial answer to this problem is to use a smooth profile for $d(x)$, ($d_{i+\frac{1}{2}} = d(h(i+\frac{1}{2}))$, as is done in the classical layers models, [17]. An alternative is to determine the best coefficients for $d(x)$ by minimizing the numerical reflection coefficients as is done in [10] for the Helmholtz equation.

# 6 Numerical Results

In the following examples, we simulate elastic wave propagation in a 2-D unbounded medium. We will present several results including the case of heterogeneous, anisotropic elastic media. In order to show the generality of the method we give some numerical results for both schemes : the Virieux finite-differences scheme and the finite-elements scheme. A more complete analysis is presented for the finite-element scheme, namely the discrete reflection coefficients are computed as a function of the incident angle. Let us first set some notation and give the characteristics of the numerical examples that will follow. We consider an unbounded domain $\Omega$ in 2D,

occupied by an elastic material and we suppose that the initial condition (or the source) is supported in a part of $\Omega$. The material will be characterized by its wave velocities $V_p$ (pressure) and $V_s$ (share) in the isotropic case and by its elasticity matrix $C$ in the anisotropic case. In order to solve numerically the elastodynamic problem in $\Omega$ we define a bounded domain $D$ of a simple geometry (here it will be a square), containing the support of the initial data, with absorbing layers (PML) on all four boundaries. For the discretisation of the problem we take a regular grid of $D$ composed by $N \times N$ square elements of edge $h = 1/N$. The time step is then computed following the CFL condition for each scheme, more precisely we take :

- $\Delta t = \dfrac{0.9h}{\sqrt{2}V_p}$ for the Virieux scheme,
- $\Delta t = \dfrac{h}{V_p}$ for the finite-elements scheme.

For our numerical experiments we use an explosive source located at the point $S = (x_1^s, x_2^s)$, that is

$$f(x,t) = F(t)\vec{g}(r) \ ,$$

with

$$F(t) = \begin{cases} -2\pi^2 f_0^2 (t-t_0) e^{-\pi^2 f_0^2 (t-t_0)^2} & \text{if } t \le 2t_0 \\ 0 & \text{if } t > 2t_0 \end{cases} \ , \tag{25}$$

$t_0 = \dfrac{1}{f_0}$, $f_0 = \dfrac{Vs}{h}\dfrac{1}{N_L}$ is the central frequency,
$N_L$ is the number of points per S wave length,

and $\vec{g}(r)$ is a radial function :

$$\vec{g}(r) = \left(1 - \frac{r^2}{a^2}\right)^3 \ 1_{B_a} \left(\frac{x_1 - x_1^s}{r}, \frac{x_2 - x_2^s}{r}\right) \tag{26}$$
$$r = \sqrt{(x_1 - x_1^s)^2 + (x_2 - x_2^s)^2}, \ a = 5h \ ,$$

with $1_{B_a}$ the characteristic function of $B_a$ the disk of center S and and radius $a$. In the absorbing layers we use the following model for the damping parameter $d(x)$

$$d(x) = d_0 \left(\frac{x}{\delta}\right)^2$$

where $\delta$ is the length of the layer and $d_0$ is a function of the theoretical reflection coefficient ($R = R_{pp}^{\delta}$) (see relation (17) for $\theta = 0$)

$$d_0 = \log\left(\frac{1}{R}\right)\frac{3V_p}{2\delta} \ .$$

We first present some results in an homogeneous isotropic medium.

## 6.1 Homogeneous, isotropic elastic medium-Virieux scheme

We consider here an elastic medium with $V_p = 2000m/s$, $V_s = 1400m/s$. The characteristics of the discretization are

$$N = 200, \ h = 0.15m, \ S = (7.5m, 7.5m),$$
$$N_L = 20, \ \delta = 10h \text{ and } R = 0.001.$$

We first present some snapshots of the solution on the normal scale in Figure 9. We can remark in the snapshots presented on Figure 9 that we can see no reflection when the results are presented on the normal scale. If we want to see some reflection we have to magnify the results. In this example the reflection coefficient is about 0.1% as we remark by magnifying the results by a factor 200 (see Figure 10).

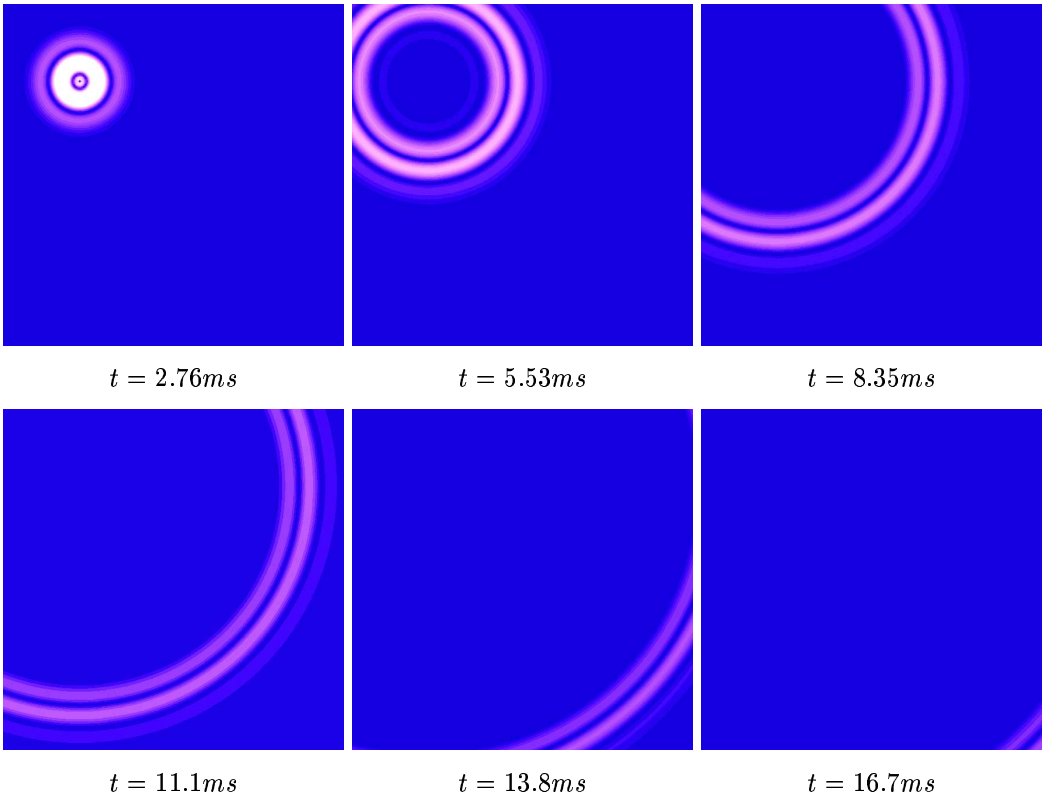


Figure 9: Snapshots of 2-D elastic finite-differences simulations, using the PML absorbing layer model. The snapshots are the norm of the velocity $\|v\| = \sqrt{v_1^2 + v_1^2}$

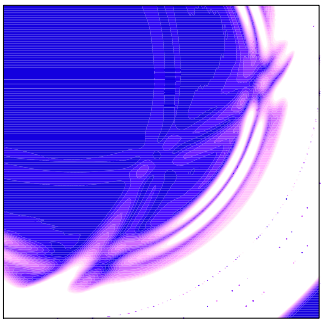

Figure 10: The snapshot at $t = 13.8ms$ magnified here by a factor 200.

## 6.2 Heterogeneous, isotropic elastic medium-Virieux scheme

We consider an heterogeneous elastic medium, the interface is parallel to the $x_1$ axis and located in the middle of the frame (see Figure 11). The wave velocities in the two media are $V_p^1 = 2000m/s$, $V_s^1 = 1400m/s$ (the upper medium), $V_p^2 = 1000m/s$, $V_s^2 = 700m/s$ (the lower medium). All the other parameters are the same as in section 6.1 where we take $V_s = (V_s^1 + V_s^2)/2$ for the computation of $f_0$ (equation 25) and $V_p = V_p^1$ to compute $\Delta t$. The source is now located in the lower medium near the interface (at point$(15m, 16.2m)$). We present some snapshots of the solution on the normal scale on Figure 11. The reflection coefficient for this example is about 0.1% as we can see on Figure 12.

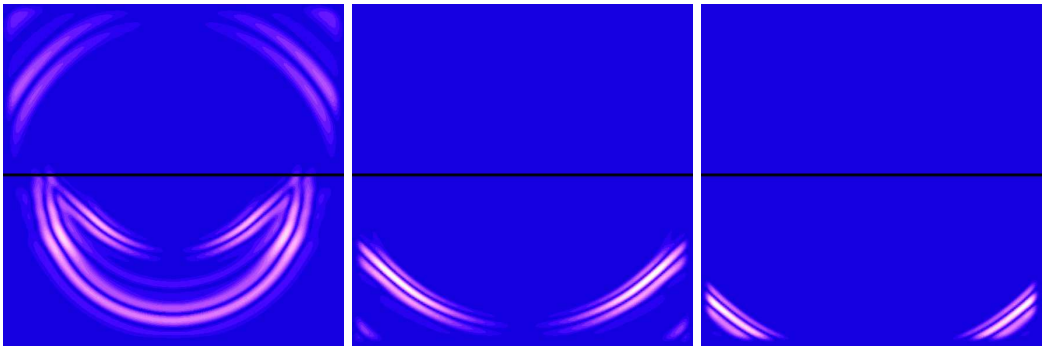

$t = 8.35ms$ $t = 13.8ms$ $t = 16.7ms$

Figure 11: Snapshots of 2-D elastic finite-differences simulations, using the PML absorbing layer model. The snapshots are the norm of the velocity $\|v\| = \sqrt{v_1^2 + v_1^2}$.

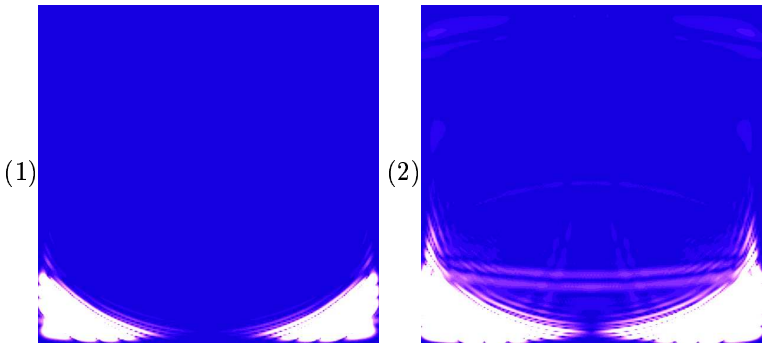


Figure 12: Snapshot of 2-D elastic finite-differences simulations, using the PML absorbing layer model. We represent here the norm of the velocity at time $t = 16.7ms$, (1) is magnified by a factor 100 and (2) by a factor 1000.

### 6.3 Heterogeneous, isotropic elastic medium. Finite-element scheme

The heterogeneous elastic medium considered here is characterized by the velocity model presented on Figure 13, we have $\frac{\max V_p}{\min V_p} = 2.1$ and $V_p = 1.6V_s$. For the discretization we take $V_p$ and $V_s$ piecewise constants (one value per element).

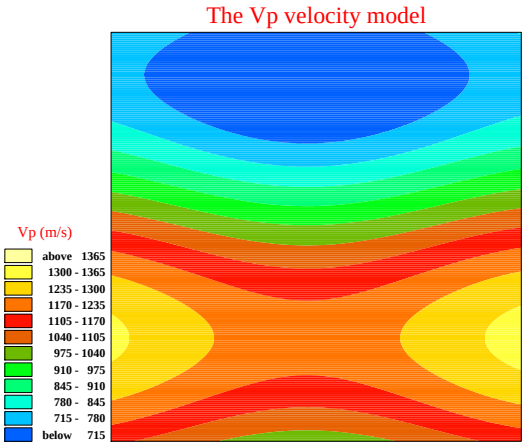


Figure 13: The velocity model for the heterogeneous medium, $\frac{\max V_p}{\min V_p} = 2.1$ and $V_p = 1.6V_s$.

The size of the grid is $200 \times 200$, $h = 0.15m$, $N_L = 10$ and the source is located at the point $(15m, 3m)$. We present, on Figure 14, three experiments with different sizes of the absorbing layer, namely, in the first we take $\delta = 5h - R = 0.01$, in the second $\delta = 10h - R = 0.001$ and finally $\delta = 20h - R = 0.0001$.

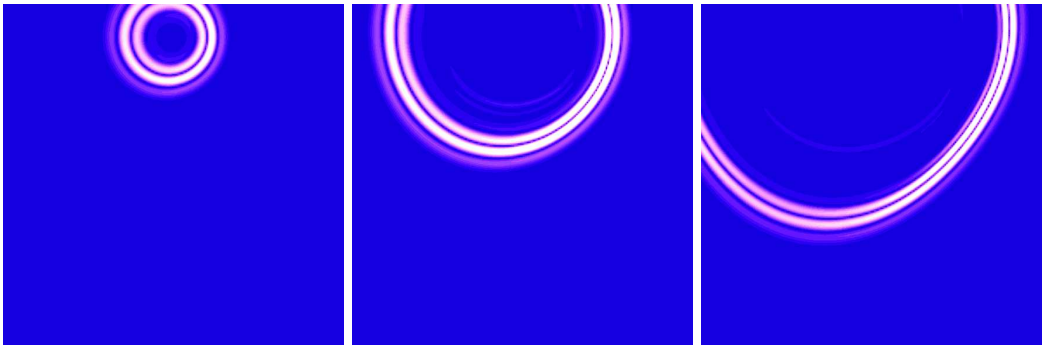

$t = 3.55ms$ $t = 7.1ms$ $t = 10.65ms$

Figure 14: Snapshots of 2-D elastic finite-elements simulations, using the PML absorbing layer model with $\delta = 5h$. The snapshots are the norm of the velocity $\|v\| = \sqrt{v_1^2 + v_1^2}$

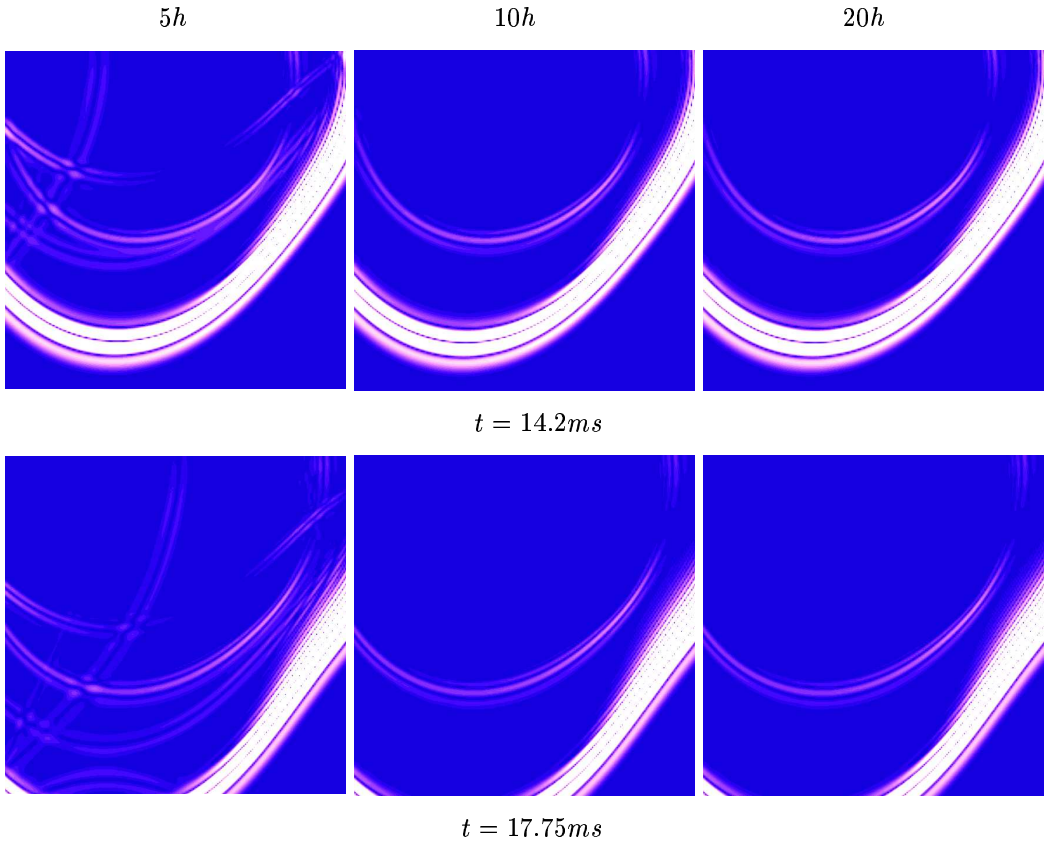


Figure 15: Snapshots of 2-D elastic finite-elements simulations, using the PML absorbing layer model with $\delta = 5h$, $\delta = 10h$ and $\delta = 20h$. All snapshots are magnified by a factor of 10.

on Figure 15 we present the snapshots of the solution magnified by a factor of 10. We remind that the reflection coefficients depend on the length of the layer, more precisely we have :

- A reflection of about 1% for $\delta = 5h$,
- a reflection of about 0.1% for $\delta = 10h$,
- and a reflection of about 0.01% for $\delta = 20h$.

These reflection coefficients which are theoretical are confirmed by the numerical examples.

## 6.4 Homogeneous, anisotropic elastic medium. Finite-element scheme

In this example we consider an anisotropic elastic solid, the apatite. We want to point out that in the case of anisotropic elastic materials only lower order absorbing boundary conditions are known and they are quite difficult to implement [2]. On the contrary the generalization of the PML model to the anisotropic case is straightforward and there are no supplementary difficulties for the implementation. Moreover the results are very satisfactory as we can see in the following Figures.

The characteristics of the problem are : $N = 200$, $h = 0.15m$, $N_L = 10$ and the source is located at the center of the frame $S = (15m, 15m)$. We present on Figure 16 three experiments, corresponding to : $\delta = 5h - R = 0.01$, $\delta = 10h - R = 0.001$ and $\delta = 20h - R = 0.0001$. We can see on Figure 16 that there is no reflection when the results are presented on the normal scale as it was already the case for an homogeneous medium. However, we can see some reflection by magnifying these results as shown on Figure 17. The reflection coefficients obtained numerically are close to the theoretical one, more precisely we obtain :

- A reflection of about 1% for $\delta = 5h$,
- a reflection of about 0.1% for $\delta = 10h$,

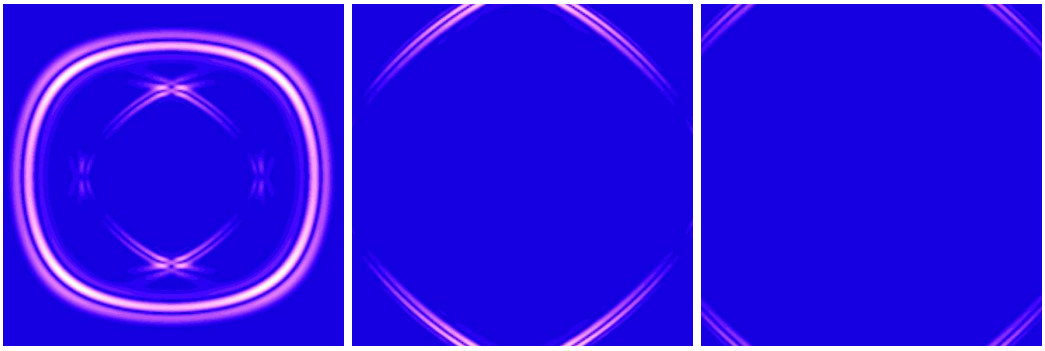

$t = 6.6ms$ $t = 13.2ms$ $t = 16.5ms$

Figure 16: Snapshots of 2-D elastic finite-elements simulations, using the PML absorbing layer model with $\delta = 5h$. The snapshots are the norm of the velocity $\|v\| = \sqrt{v_1^2 + v_1^2}$

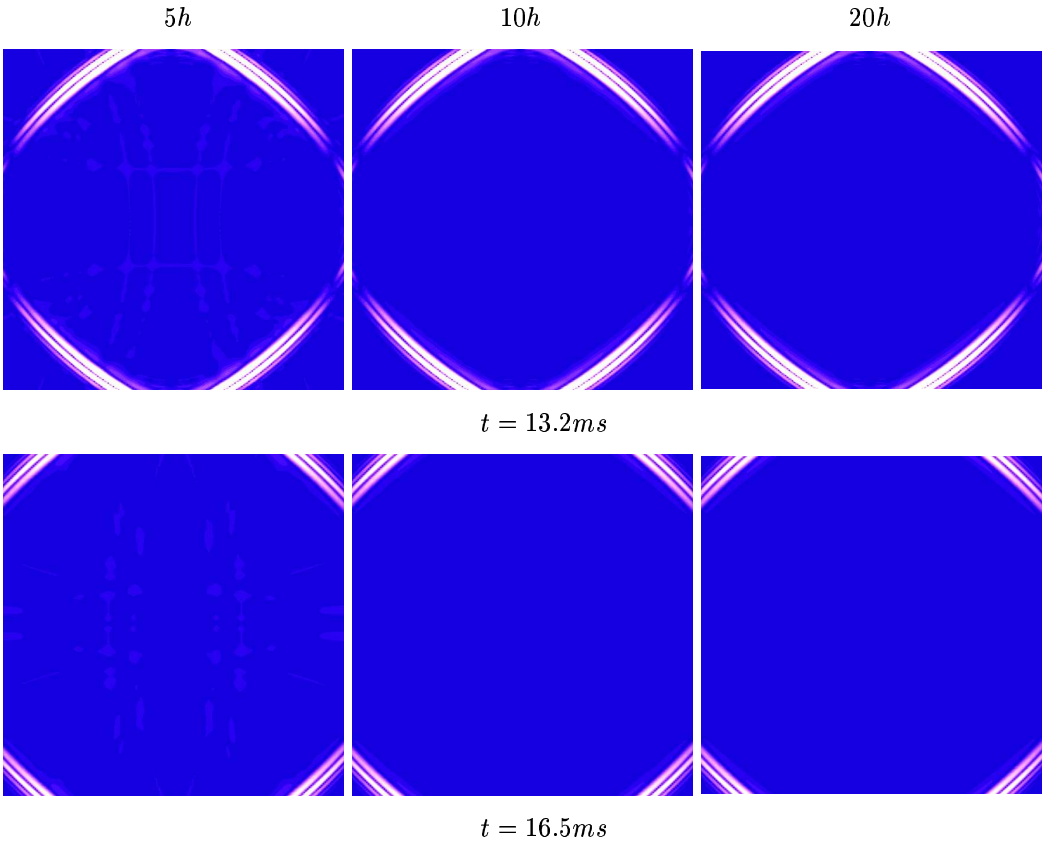


Figure 17: Snapshots of 2-D elastic finite-elements simulations, using the PML absorbing layer model with $\delta = 5h$, $\delta = 10h$ and $\delta = 20h$. The snapshots are the norm of the velocity $\|v\| = \sqrt{v_1^2 + v_1^2}$ magnified by a factor 10.

- and a reflection of about 0.02% for $\delta = 20h$.

## 6.5 Reflection Coefficients

In this section we present reflection coefficients computed using numerical simulations. We consider an homogeneous isotropic elastic solid ($V_p = 5.710m/s$, $V_s = 2.93m/s$) and we use the finite-element scheme for the space discretization.

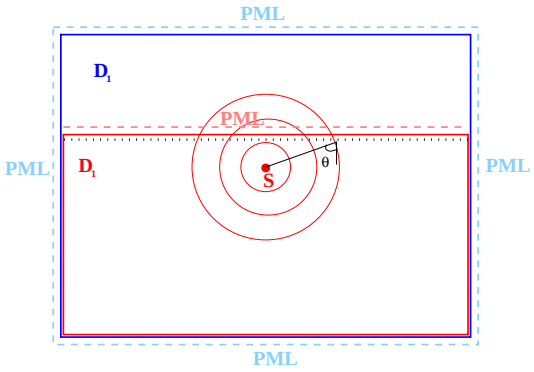


Figure 18: Geometry for computing reflection coefficients.

Figure 18 shows the geometry of the problem consisting of two computational domains $D_1$ and $D_2$. To compute the reflection coefficient we consider the solution at points near the upper boundary of $D_1$ as shown on Figure 18. Denoting by $(U_1)_i$(resp. $(U_2)_i$) the velocity at point $M_i$ in $D_1$(resp. $D_2$) we take

$$(R_{pp})(\theta_i) = \frac{\mathrm{div}(U_2)_i - \mathrm{div}(U_1)_i}{\mathrm{div}(U_2)_i}$$
$$(R_{ps})(\theta_i) = \frac{\mathrm{curl}(U_2)_i - \mathrm{curl}(U_1)_i}{\mathrm{curl}(U_2)_i} \quad . \tag{27}$$

That is the expression for the reflection coefficients in the case of a pure P-wave source. In the same way we can define

$$(R_{ss})(\theta_i) = \frac{\mathrm{curl}(U_2) - \mathrm{curl}(U_1)}{\mathrm{curl}(U_2)}$$
$$(R_{sp})(\theta_i) = \frac{\mathrm{div}(U_2) - \mathrm{div}(U_1)}{\mathrm{div}(U_2)} \quad ,$$

in the case of a pure S wave source. For our examples we use a P-wave source function described by (25,26) with $N_L = 16$. For this source function the rotational of the velocity is smaller then the divergence by a factor $10^{-10}$ so that the reflection coefficient $R_{ps}$ is negligible.

**Remark 3** *Relation 27 is used to compute reflection coefficients at each time step, to obtain results presented on Figure 19 we integrate over time.*

The grid size is $400 \times 200$ for $D_1$, $400 \times 300$ for $D_2$ and $h = 0.5m$ for both domains. The source is located at point $(200, 80)$ of the grid. As we can see on Figure 18 the domain is surrounded by absorbing layers, in which we take

$$d(x) = d_0 \left(\frac{x}{\delta}\right)^4 \tag{28}$$

where $\delta$ is the length of the layer and $d_0$ is given by

$$d_0 = \left|\log\left(\frac{1}{R}\right)\right| \frac{4V_p}{2\delta} \quad .$$

We present three experiments with $\delta = 5h - R = 10^{-4}$, $\delta = 10h - R = 10^{-6}$ and $\delta = 20h - R = 10^{-8}$. To examine the performance of the PML model, comparisons with the 1st, 2nd and 3rd order Higdons absorbing boundary conditions are presented.

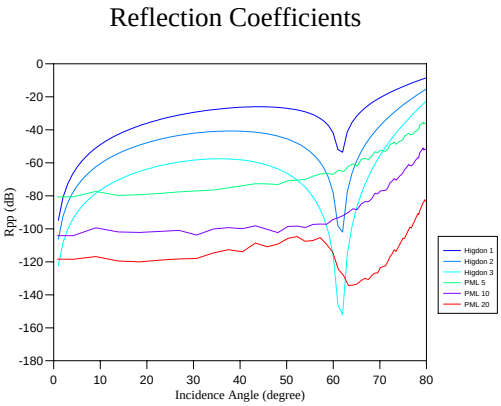


Figure 19: Comparison of $R_{pp}$ for the Higdon ABC's and PML.

**Remark 4** *The reflection coefficients for the absorbing boundary conditions proposed by Higdon are the theoretical ones. We obtain them by applying an operator of the form*

$$\prod_{i=1}^{m} \left( \beta_i \frac{\partial}{\partial t} + V_p \frac{\partial}{\partial n} \right) \ .$$

*For the example we have taken*

- *For* $m = 1$ *:* $\beta_1 = 1$,
- *For* $m = 2$ *:* $\beta_1 = 1$, $\beta_2 = V_p/V_s (= 1.95)$,
- *For* $m = 2$ *:* $\beta_1 = 1$, $\beta_2 = 1.5$ *and* $\beta_3 = V_p/V_s (= 1.95)$.

As we can see on Figure 6.5 for almost all angles of incidence the PML absorbing layer model gives better results then the absorbing boundary conditions of first and second order and this even for the $5h$ length absorbing layer. Compared to the third order absorbing condition the PML layers of $10h$ and $20h$ are substantially better except near the $60°$ degree angle. We want to point out that in this example we compare the reflection coefficients provided by the continuous Higdon model to the one given by the discrete PML model. It is known that the Higdon reflection coefficients increase when discretization is used.

The numerical results presented in sections 6.1, 6.2, 6.3, 6.4 and 6.5 show the generality of the PML model which can be easily applied in several numerical schemes and gives satisfactory results even in the case of anisotropic heterogeneous elastic media. The reflection coefficients are near the theoretical ones for all the presented experiments, so we can resume the following : For the considered models of the damping factor the reflection coefficients are about 1% for a $5h$ PML layer length, below 0.2% for a $10h$ PML layer length and below 0.1% for a $20h$ PML layer length for all experiments. In practice one should choose the length of the layer as a function of the scale of the problem and the requested reflection coefficient. In the numerical examples that we have presented the scale of the problems was about 15 wavelengths of P-wave ($\lambda_p$) in each direction, in this case a PML layer with $\delta = 5h$ (that is about 0.5 $\lambda_p$) is sufficient and gives better results than the second order absorbing condition. However, for larger scale computations the numerical dispersion will be more important and thus a PML layer with $\delta = 5h$ would probably not give the expected results. Thus for large scale problems one should consider a PML layer with $\delta \geq 10h$. We want to point out, that even in this case the additional cost remains modest, given that the layer only represents a small portion of the total grid. Let us finally remark that the PML model can be easily extended to the case of Rayleigh waves. (Experimental results not shown in this paper have demonstrated a good absorbtion of Rayleigh waves).

# 7 Conclusions

We have presented in this paper a generalization of the PML absorbing layer model for the elastodynamic problem in the case of heterogeneous, anisotropic media. The implementation of this model was presented in the 2D case but it can be straightforwardly extended to the 3D case. The superiority of this model compared

to the absorbing boundary conditions proposed by Higdon was shown by numerical results in the case of an isotropic homogeneous medium. Moreover we have shown by several numerical examples the efficiency of this model : remarkable results even in the case of heterogeneous, anisotropic media. Finaly we want to point out the ease of the generalization and the implementation of this model in the case of an anisotropic elastic medium in comparison with the complexity of the respective absorbing boundary conditions.

# References


[1] B. A. Auld. *Acoustic Fields and Elastic Waves in Solids*, volume I et II. Wiley, 1973.

[2] E. Bécache. *Résolution par une méthode d'équations intégrales d'un problème de diffraction d'ondes élastiques transitoires par une fissure.* PhD thesis, PARIS 6, 1991.

[3] E. Bécache, P. Joly, and C. Tsogka. Eléments finis mixtes et condensation de masse en élastodynamique linéaire. (i) construction. *C.R. Acad. Sci. Paris*, t. 325, Série I:545–550, 1997.

[4] E. Bécache, P. Joly, and C. Tsogka. Fictitious domain method applied to the scattering by a crack of transient elastic waves in anisotropic media : a new family of mixed finite elements leading to explicit schemes. pages 322–326. SIAM, 1998.

[5] J.P. Bérenger. A perfectly matched layer for the absorption of electromagnetic waves. *Journal of Comp. Physics.*, **114**:185–200, 1994.

[6] J.P. Bérenger. Three-dimensional perfectly matched layer for the absorption of electromagnetic waves. *Journal of Comp. Physics.*, **114**(2):363–379, 1996.

[7] J.P. Bérenger. Improved PML for the FDTD Solution of Wave-Structure Interaction Problems . *IEEE transactions on Antennas and Propagation.*, **45**(3):363–379, march 1997.

[8] B. Chalindar. *Conditions aux limites artificielles pour les équations de l'élastodynamique.* PhD thesis, Saint Etienne (France), 1987.

[9] F. Collino. Perfectly matched absorbing layers for the paraxial equations. *J. of Comp. Phy.*, (131):164–180, 1996.

[10] F. Collino and P.B. Monk. Optimizing the perfectly matched layers. *Comput. Methods Apl. Mech. Engrg.*, pages –, to appear 1998.

[11] B. Engquist and A. Majda. Absorbing boundary conditions for the numerical simulation of waves. *Math. Comp.*, 31(139):629–651, Juillet 1977.

[12] T. Hagstrom. On high-order radiation boundary condition. In B. Engquist and G. A. Kriegsmann, editors, *Computational Wave Propagation*, volume 86 of *The IMA Volumes in Math. and Applications*. Springer, 1997.

[13] F. Hastings, J.B. Schneider, and S. L. Broschat. Application of the perfectly matched layer (PML) absorbing boundary condition to elastic wave propagation . *J. Acoust. Soc. Am.*, **100**(5):3061– 3069, November 1996.

[14] R.C. Higdon. Absorbing boundary conditions for elastic waves . *Geophysics.*, **56**( 2):231–241, February 1991.

[15] R.L. Higdon. Radiation boundary conditions for elastic wave propagation. *SIAM J. Numer. Anal.*, 27(4):831–870, April 1990.

[16] R.L. Higdon. Absorbing boundary conditions for acoustic and elastic waves in stratified media. *J. Comput. Phys.*, 101(2):386–418, 1992.

[17] M. Israeli and S.A. Orszag. Approximation of radiation boundary conditions. *Journal of Comp. Physics.*, **41**:115–135, 1981.

[18] C. Peng and M.N. Toksoz. An optimal absorbing boundary condition for elastic wave modeling . *Geophysics.*, **60** (1):296–301, January-February 1995.

[19] C. M. Rappaport. Perfectly matched absorbing conditions based on anisotropic lossy maping of space. *IEEE Micr. Guid. Wave Lett.*, 5(90), 1995.

[20] A. Simone and S. Hestholm. Instability in applying absorbing boundary conditions to high-order seismic modeling algorithms . *Geophysics.*, **63**( 3):1017–1023, May-June 1998.

[21] J. Sochacki, R. Kubichek, J. George, W.R. Fletcher, and S. Smithson. Absorbing boundary conditions and surface waves . *Geophysics.*, **52** (1):60–71, January 1987.

[22] J. Virieux. P-sv wave propagation in heterogeneous media :velocity-stress finite difference method. *Geophysics*, 51(4):889–901, 1986.

[23] L. Zhao and A.C. Cangellaris. A general approach to for developping unsplit-field time-domain implementations of perfectly matched layers for FDTD grid truncation. *IEEE trans. Microwave Theory Tech..*, **44**:2555–2563, 1996.

Unit´e de recherche INRIA Lorraine, Technopôle de Nancy-Brabois, Campus scientifique,
615 rue du Jardin Botanique, BP 101, 54600 VILLERS LÈS NANCY
Unit´e de recherche INRIA Rennes, Irisa, Campus universitaire de Beaulieu, 35042 RENNES Cedex
Unit´e de recherche INRIA Rhône-Alpes, 655, avenue de l'Europe, 38330 MONTBONNOT ST MARTIN
Unit´e de recherche INRIA Rocquencourt, Domaine de Voluceau, Rocquencourt, BP 105, 78153 LE CHESNAY Cedex
Unit´e de recherche INRIA Sophia-Antipolis, 2004 route des Lucioles, BP 93, 06902 SOPHIA-ANTIPOLIS Cedex

Éditeur
INRIA, Domaine de Voluceau, Rocquencourt, BP 105, 78153 LE CHESNAY Cedex (France)
http://www.inria.fr
ISSN 0249-6399